



Fire across frontiers: Satellite-based investigation of climate-fire interactions in the Middle East (West Asia)

Wan Ni Lin^{1,2}, Abdulhakim M. Abdi^{1,2}, Lina Eklund^{1,2,3}

¹Department of Earth and Environmental Sciences, Lund University, Sölvegatan 12, 223 62, Lund, Sweden

5 ²Centre for Advanced Middle Eastern Studies (CMES), Lund University, 22362, Lund, Sweden

³United Nations University, Institute for Water, Environment and Health (UNU-INWEH), 225 East Beaver Creek Road, Richmond Hill, ON, L4B 3P4, Canada

Correspondence to: Wan Ni Lin (wan_ni.lin@mgeo.lu.se)

Abstract. Although the global burned area has declined in recent decades, fire activity worldwide is projected to become more frequent and intense due to both climate change and human activities, including fire ignition, suppression and land use changes. In the Middle East (West Asia), climate change, rapid urbanisation, cropland expansion and armed conflict impacts all play a part in the increased risk of fire. While this region has experienced several large-scale fires over the last decade, little research has focused on regional and cross-border fire dynamics and their links to climate and other biophysical factors. This study aims to fill this gap by investigating vegetation fire dynamics across Turkey, Syria, Iraq, Iran, Lebanon, Israel and Palestine between 2001 and 2022.

We assessed long-term spatio-temporal fire trends using satellite-derived active fire and burned area products. To explore the relationship between potential factors and fire activity, we used Spearman Rank Correlation to quantify the correlation between annual burned area, active fire, climate, topography and population density. Our results reveal a prominent arc-shaped transboundary fire pattern crossing international borders, with fire risk frequently concentrated along the boundaries between neighbouring countries (Turkey, Syria, Iraq and Iran). Crucially, the data show that 74 per cent of the total burned area occurred on croplands, underscoring the dominance of humans in the fire regime. Regional climate and population density show only weak or limited associations with annual active fires and burned area. While topographic factors show a stronger correlation, this relationship is largely indirect, reflecting the fact that intensive agricultural burning is concentrated in flatter, more accessible areas. This study advances understanding of fire dynamics in the Middle East and further supports more effective fire risk mitigation and preparedness in the future.

1 Introduction

The Middle East (West Asia)¹, a predominantly dryland region renowned for limited water resources and high temperatures, often experiences hazards such as droughts, dust storms, heatwaves and vegetation fires. Among these, fires remain an

¹ 'Middle East' is a geopolitical term that usually refers to countries in the Levant region, together with Iran, Turkey, Egypt and the Arabian Peninsula. Originating from 18th-century British naval strategy for bases between Suez and Singapore, both 'Middle East' and 'Near East' have been criticised as Eurocentric terms that define regions by their distance from Europe, rather than recognising their own geographic or cultural identities.



understudied topic as they involve complex interactions between climate, ecological systems and human activities across semi-
30 arid, arid and Mediterranean-type climates. Remarkably, 83 per cent of vegetation fires in the Middle East occur on agricultural
land (Chen et al., 2023), thereby reflecting the region's predominantly dryland character, where sparse natural vegetation
makes croplands the primary fuel source. However, these agricultural fires pose significant risks to adjacent forests,
particularly in Mediterranean climate zones where denser vegetation provides continuous fuel pathways. As extreme
35 heatwaves and prolonged droughts intensify (Zittis et al., 2022), studies in the Middle East also suggest that agricultural fires
may increase the risk of larger fire hazards (Eskandari & Chuvieco, 2015; Sabancı, 2025). Furthermore, human exposure to
wildfires has been rising in recent years due to greater spatial overlap between wildland fires and human settlements (Seydi et
al., 2025). For instance, the massive wildfires in southern Turkey during the summer of 2021 burned more than 206,013 ha of
land, resulting in eight fatalities and destroying forests, farmlands and villages (Acar & Gonencgil, 2023; Aydin-Kandemir &
Demir, 2023). Similarly, the 2019–2020 fires that devastated agricultural areas in Syria's Al-Hasakah and Hama regions
40 resulted from complex interactions between conflict, migration, climate and land use changes (Zubkova et al., 2021).

Fire behaviour is controlled by three factors: fuel, weather and topography. In the Middle East, Mediterranean vegetation
comprising flammable pine and shrub species serves as the primary fuel source in addition to crop residues. Brutia pine (*Pinus*
brutia) and Aleppo pine (*Pinus halepensis*) provide significant fuel loads for large vegetation fires in Mediterranean coniferous
45 forests (Kint et al., 2014; Ne'eman & Osem, 2021). In addition, Mediterranean maquis, with a mix of various shrub species
(*Cistus*, *Pistacia lentiscus* and *Rosmarinus officinalis*), are not only flammable; they are also strongly responsive to interannual
climate variability, which dictates their biomass accumulation and moisture content (Baudena et al., 2020; Pellizzaro et al.,
2007). This makes them the key mediators through which climate fluctuations translate into fire risk (Salis et al., 2016).

50 While vegetation provides the fuel for fire, climate determines how this fuel accumulates, ignites and spreads. Warm, dry
weather typically reduces the fuel moisture content, rendering vegetation more susceptible to ignition. Beyond these short-
term weather effects, fire hazards in Mediterranean ecosystems are also driven by a climate time-lag effect in which antecedent
wet conditions in previous years promote the growth of fine fuels, which then dry out during subsequent droughts to create
high-intensity fire (AghaKouchak et al., 2020; Marriner, 2013). This interannual climate mechanism is evident in recent
55 extreme fire events. For instance, the 2021 megafire in Turkey was primarily caused by arson, but was intensified by abundant
fuel linked to a positive precipitation anomaly in 2019 (Ekberzade et al., 2025). In Israel, several studies have shown that fuel
availability from antecedent wet conditions contributes to summer fires, while fuel flammability due to prolonged drought
plays a key role in spring and autumn fires (Turco, Levin, et al., 2017; Wittenberg & Kutiel, 2016). This critical role of past

In this study, we adopt the term 'Middle East (West Asia)' to describe our study area and scope: Turkey, Syria, Iraq, Iran, Lebanon, Israel and Palestine. This term acknowledges the widespread recognition of 'Middle East' in current academic and policy disclosure while also incorporating 'West Asia' to reflect geographic accuracy and a decolonial perspective.



precipitation in shaping future fire risk is consistent across other Mediterranean climate regions globally, including Spain, Greece, France and western USA (Jones et al., 2022; Koutsias et al., 2013; Pilliod et al., 2017; Turco, Von Hardenberg, et al., 2017).

In addition to climate and vegetation, topography is an important factor that remains stable over time yet affects fuel distribution, human accessibility, wind exposure and fire spread patterns. Topography can directly affect fire spread, especially on steep slopes where fuels are more readily preheated and winds may be accelerated. Examples can be observed from large fires in Iran's semi-arid oak forests (Sadeghi et al., 2025) and Turkey, where areas of high burn severity were reported on moderately steep slopes (Genç et al., 2023). In steep terrain, slopes are often unsuitable for most agricultural activities in the Middle East, which may lead to accumulation of fuel. Furthermore, human access for both ignition and suppression is reduced. The aspect of the slope can exacerbate these patterns by creating microclimatic contrasts, as south-facing slopes experience higher temperatures and lower fuel moisture, thereby increasing fuel combustibility as set out above (Mermoz et al., 2005; Novo et al., 2024). In addition, fires are more common at lower elevations due to higher temperatures and proximity to settlements and agricultural activity, though high-altitude shrublands within wildland-urban interfaces also experience elevated fire risk (Calviño-Cancela et al., 2017). In summary, topographic factors influence the fire regime by mediating interaction between fuel conditions, weather patterns and ignition sources.

While biophysical factors may create conditions that allow fire to spread, 90 per cent of fires are ignited by humans through actions such as land use and management practices, arson and carelessness (Ekberzade et al., 2025; Jain et al., 2020). Anthropogenic factors such as population density, fire management policy, economy, resource allocation and conflicts can also alter fire behaviour directly or indirectly. Direct anthropogenic fires include stubble burning during harvest seasons (Velayati et al., 2024), intentional land clearing, military activities and arson. Indirect drivers include land use changes that create increased fuel loads, lack of suppression capacity due to weak governance, and conflict-related disruptions to traditional fire management practices. For example, fire risk patterns and fuel distribution were substantially altered in Iraq's Sulaymaniyah Province, where built-up areas increased by 419 per cent and agricultural fallow areas increased by 226 per cent between 1988 and 2017 (Khwarahm, 2021). Ignition can be triggered through bombing and military operations, as experienced across Turkey, Syria and Iraq, where armed conflicts coincide with increased fire activity (Dinc et al., 2021; Eklund et al., 2021; Eklund & Dinc, 2024; Jaafar et al., 2022; Zubkova et al., 2021). However, human activities do not necessarily increase the burned area (BA); instead, they may also reduce the BA through changing fire management strategies, fire suppression or urban land expansion that creates firebreaks (Andela et al., 2017).

In the Middle East, research on fires regimes has largely been carried out in countries such as Turkey, Israel, Iran and Lebanon (Ardakani et al., 2011; Guk et al., 2023; Majdalani et al., 2022; Memisoglu Baykal, 2023). However, these studies focus primarily on national scale, despite the fact that fires can be transboundary hazards (Miller et al., 2022; Pismel et al., 2023).



We argue that there are three main motivations for performing a regional fire assessment. First, climate drivers of vegetation fire, such as heat, dryness and wind, are controlled by large-scale atmospheric circulation systems that operate across national boundaries, providing fire-conducive conditions over multiple countries (Gandham et al., 2025). Second, countries in the Middle East share similar types of fuel, including Mediterranean forests, shrubs and agricultural residues, thereby creating a regional fuel pattern. Third, many fires linked to armed conflict frequently occur near borders, underscoring the importance of examining transboundary fire activity. Given the ecological sensitivity and social vulnerability of the region's dryland ecosystems, where fire regimes are increasingly shaped by agricultural activities, climate change and armed conflict, there is a critical need for a long-term, region-wide assessment of vegetation fire dynamics in the Middle East. A further gap in existing research concerns the time-lagged moisture–fire relationship; although this mechanism is well documented in other Mediterranean-climate regions, it remains insufficiently characterised across the Middle East. By examining fire occurrence patterns and their relationships with climate variables, we seek to understand the drivers and factors influencing regional fire activity. This study aims to provide a comprehensive analysis of spatial and temporal fire patterns across the Middle East from 2001 to 2022. Focusing on Turkey, Syria, Iraq, Iran, Lebanon, Israel and Palestine, spanning Mediterranean, arid and semi-arid climates, we examine fire trends and their connections to climatic and anthropogenic drivers. Ultimately, this research expects to inform more effective, regionally coordinated fire management and policy responses.

This study aims to provide an overview of vegetation fires in the Middle East between 2001 and 2022 in terms of spatio-temporal perspectives, examining climatic variability, topographic factors and anthropogenic influences. Encompassing Turkey, Syria, Iraq, Iran, Lebanon, Israel, and Palestine, the research addresses critical gaps in transboundary fire analysis and explores the time-lagged relationships between antecedent moisture conditions and fire occurrence; a dimension that remains underexplored in this region. These objectives will be achieved by addressing the following research questions:

1. How do fire occurrence and burned area vary spatially and temporally across different land cover types in the Middle East?
2. How do climatic, topographic and anthropogenic variables co-occur to shape regional fire occurrence and burned area patterns?
3. To what extent do antecedent precipitation patterns exhibit time-lagged relationships with fire activity across the diverse ecosystems in the region?

2 Data and methods

2.1 Study area

This study focuses on Turkey, Syria, Iraq, Iran, Lebanon, Israel and Palestine, spanning approximately 25°N to 42°N latitude and 26°E to 63°E longitude and covering a total area of 3,064,062 km² (Figure 1). The region is characterised by dry sub-humid, semi-arid and arid lands, with hot, dry summers and mild, wet winters. Inter-annual temperature and precipitation



125 variability is influenced by complex atmospheric circulation patterns, topography and proximity to major water bodies, shaping
spatially heterogeneous fire regimes. The western part of the study area experiences a Mediterranean climate, receiving more
than 400 mm of rainfall annually and over 1,000 mm in mountainous areas such as the Taurus, East Anatolian Mountains, the
Zagros Mountains, Anti-Lebanon and the Caspian Sea region, supporting the fuel production of coniferous forests and dense
shrublands that generate substantial fuel loads. By contrast, desert regions in southern Iraq, Syria and Iran receive less than
130 100 mm of rainfall per year (Frumkin & Shtober-Zisu, 2024), limiting fuel continuity and biomass accumulation. The timings
of wet seasons and dry seasons vary across regions; but generally the area receives most of its rainfall in winter and spring
(October to April), and summer temperatures frequently exceed 40 °C (Rousta et al., 2021). This seasonality drives fire risk:
fuels accumulate during winter–spring rains and then cure during the prolonged dry season in summer, thereby resulting in
distinct fire seasonality across the region. For example, the fire season in Turkey extends between May and September
135 (Ertugrul et al., 2021); while in Northern Iran, it occurs between May and October (Ardakani et al., 2011).
Land cover (LC) reflects the region’s predominant aridity, with bare land comprising 45 per cent of the area, representing fuel-
limited zones where fire spread is naturally constrained. Grasslands (26 per cent) provide fine, continuous fuels that support
fast-spreading fires, while croplands (12 per cent) fragment natural fuel continuity but provide human ignition sources through
residue burning, for example. Mediterranean woodlands and shrublands, though spatially limited to more humid zones, support
140 the highest fuel loads and most intense fire behaviour; ranging from pine forests and shrublands in Turkey to extensive oak
woodlands across the Zagros Mountains (Bilgili & Saglam, 2003; Rasooli et al., 2021). Agricultural systems consist of wheat–
barley cereal production, cotton cultivation, olive groves, vineyards and orchard systems, all of which play important roles in
rural livelihoods and in shaping fire ignition patterns. Human activities ranging from pastoral grazing and residue burning to
land clearing and conflict-related disturbances contribute additional layers of complexity to the region’s fire dynamics.

145

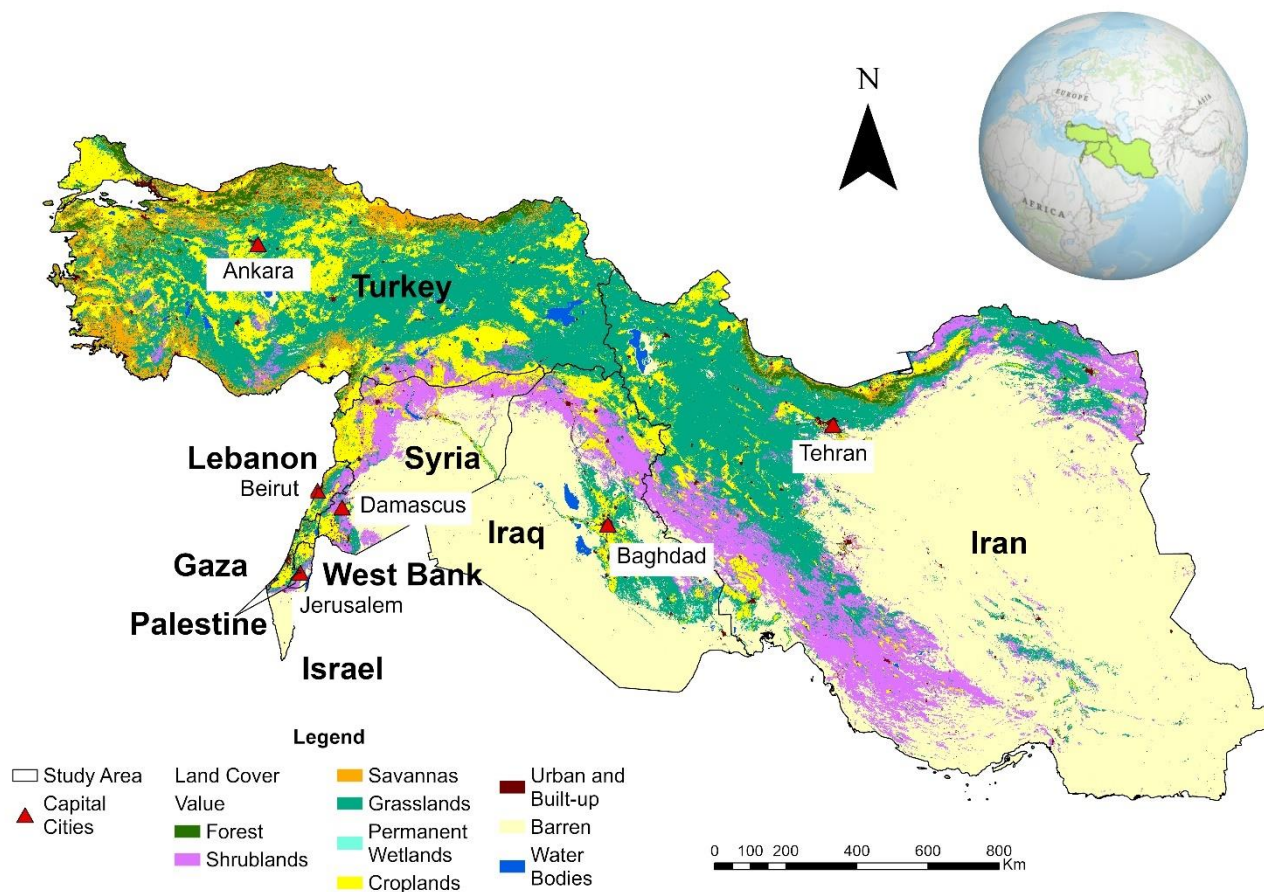


Figure 1: Land cover map of the study area in the Middle East, showing distribution of land cover types and capital cities. Land cover data: MODIS MCD12Q1.061 (2022); Capital Cities: populated places data, Natural Earth (2009).

2.2 Data

150 Understanding the fire regime requires information about fire occurrence, climate, vegetation, and human and environmental factors. Therefore, we compiled multiple data sources to capture drivers of vegetation fires in the Middle East. The datasets selected represent (i) fire occurrence and extent, (ii) climate variability and water balance, (iii) land cover and vegetation productivity (fuel type and amount) and (iv) topographic and demographic factors that shape fire ignition, spread and suppression. This data compilation enables a systematic assessment of the drivers of regional fire dynamics in the Middle East
155 from 2001 to 2022 (Table 1).



2.2.1 Fire data

Earth observation satellites are an indispensable tool for monitoring fire dynamics, particularly in regions where in-situ reporting is inconsistent or inaccessible (Chuvienco et al., 2019). To improve the robustness of fire detection, we combine two MODIS fire products: MCD64A1 for burned area (BA) mapping and MCD14ML for active fire (AF) detections. This strategy
160 allows us to capture fire activity consistently over the twenty-two years using both types of information. Accurate fire assessment requires high temporal and spatial resolution, as BA may be under-detected when fires leave little residual heat, spread rapidly in the interval between satellite passes or produce minimal pre- and post-fire spectral change (Hawbaker et al., 2008). While the ESA Fire Climate Change Initiative (FireCCI51) product offers advantages in detecting smaller (<100 ha) fires compared to MCD64A1 (Katagis and Gitas, 2022), its temporal coverage is limited to 2001–2020, making it unsuitable
165 for this study.

The MCD64A1 dataset is generated using a hybrid algorithm that combines a burn-sensitive vegetation index, derived from MODIS surface reflectance, with MODIS AF detections (Giglio et al., 2009). On the other hand, MODIS AF data are based on thermal anomalies, providing near-real time fire point data that can capture fire occurrences more rapidly. We used Google
170 Earth Engine (GEE) (Gorelick et al., 2017) and the Fire Information for Resource Management System (FIRMS) to obtain BA and AF data, respectively. We filtered BA data for high-confidence burn dates and AF data with confidence levels exceeding 80 per cent, excluding volcanoes, static sources and offshore detections.

2.2.2 Climate and vegetation data

We used the Standardised Precipitation-Evapotranspiration Index (SPEI) to capture combined effects of precipitation and
175 temperature on water balance (Vicente-Serrano et al., 2010). SPEI has been used to evaluate climate and fire relationships in several studies, showcasing its ability to understand the connection between fuel moisture, fuel accumulation and fire in Mediterranean, arid and semi-arid regions (McEvoy et al., 2019; Turco, Levin, et al., 2017). SPEI is a multi-scalar index that can be calculated over different accumulation periods, enabling the assessment of drought impacts across seasonal to interannual timescales.

180 We calculated SPEI over multiple temporal scales and seasonal partition in order to characterise fuel moisture and fuel accumulation relevant to fire activities. Although the timing of wet and dry periods varies from country to country, we defined two broad seasons to represent winter moisture-driven fuel accumulation and summer fuel desiccation. Therefore, nine SPEI variables were calculated: SPEI-3 for wet seasons (October to April) and dry seasons (May to September) (minimum, mean, median and maximum values for each). Furthermore, to explore the influence of long-term water balance on subsequent fire
185 activity, we include SPEI12, accumulating SPEI from the past twelve months, which allows us to test lagged climate–fire relationships whereby wet years increase fuel availability and elevate fire risk in subsequent dry periods. The data are extracted



from the work of Gebrechorkos et al.(2023), using global SPEI data with 5 km resolution based on the CHIRPS_GLEAM model.

Annual vegetation productivity was assessed using NDVI from combined MODIS Terra (MOD13A1) and Aqua (MYD13A1) products, calculated as annual sums to represent fuel accumulation potential (Abel et al., 2020) and its influence on AF and BA and spread through fuel accumulation.

2.2.3 Topography data

Topographic variables were derived from the Advanced Spaceborne Thermal Emission and Reflection Radiometer (ASTER) Global Digital Elevation Model (GDEM), Version 3 at 30 m spatial resolution (Abrams et al., 2022). We calculated elevation, slope and aspect using the GEE terrain function and included these variables to account for their influence on fire behaviour through effects on microclimate, fuel moisture, vegetation distribution, fire spread and human accessibility.

2.2.4 Population data

Population density was included as a spatial proxy for human influence on AF and BA in the Middle East, representing both potential ignition sources (agricultural burning, land management and accidental ignitions, for example) and fire suppression capacity. We used population density data from the WorldPop research programme (Bondarenko et al., 2020), selecting the population density map for 2020 using constrained top-down estimation modelling. This method used satellite-based data together with settlement and buildings maps to disaggregate the population into 100 m grid cells, estimating population distribution based on building locations. This has been suggested to be suitable for estimating rural populations. Although gridded population datasets are known to underestimate population in dense and informal settlements and show reduced accuracy at cell level (Thomson et al., 2022), they remain suitable for regional-scale analyses where population is used as a proxy for human influence rather than absolute demographic counts. Accordingly, this dataset provides a spatial representation of human presence for examining broad patterns of anthropogenic influence on fire activity across the Middle East. While population count is dynamic between 2001 and 2022, the 2020 constrained dataset was selected as a stable proxy for the regional settlement distribution and wildland-urban interface. We prioritise the high spatial resolution of the 2020 constrained model over the temporal variability of the unconstrained annual products, as the former better provides a broad picture of human–fire interactions.

2.2.5 Land cover data

We used the MODIS LC product (MCD12Q1.061), a global product that spans the period from 2001 to the present day, to ensure temporal consistency with the fire dataset. Despite its coarse resolution and known limitations in heterogeneous landscapes where grasslands, croplands and barren areas are difficult to distinguish (Li et al., 2017), MODIS LC provides one of the few continuous, long-term and broad-coverage datasets available for the Middle East. An accuracy assessment in northern Iran reported an overall accuracy of 75 per cent, with dense forest classified most reliably (~95 per cent), while natural



herbaceous cover and shrublands showed lower accuracy (Jahromi et al., 2021). Given the lack of comparable regional products, MODIS LC offers a practical baseline for analysing land cover dynamics in relation to fire.

220 **Table 1: Input variable characteristics.**

Data type	variables	Time period	Original spatial resolution	Data name/source
Fire	Active fire (AF)	2001–2022	1 km	MCD14ML (Giglio et al., 2016)
	Burned area (BA)		500 m	MCD64A1 (Giglio et al., 2009)
Climate	SPEI12		5 km	Gebrechorkos et al.(2023)
	SPEI 3 (wet)			
	SPEI 3 (dry)			
Topography	Elevation		2020	30 m
	Slope			
	Aspect			
Vegetation	NDVI sum	2001–2022	500 m	MODIS MOD13A1 (Terra), MYD13A1 (Aqua)
Population		2020	100 m	WorldPop (Bondarenko et al., 2020)
Land cover		2001–2022	500 m	MCD12Q1.061 (Friedl & Sulla-Menashe, 2022)

2.3 Method

2.3.1 Time-series visualisation

Using MODIS AF, BA and LC data, our aim is to examine annual trends in AF and BA across the different LC types and affected regions between 2001 and 2022. During this process, we merged water bodies, urban and built-up areas and permanent snow and ice into a single class labelled ‘Other’ as they constitute only a minor portion of areas with AF/BA. These classes may also reflect spatial misalignments between datasets, classification errors in the MODIS LC product or false-positive detections (commission errors) in the AF/BA products (such as sun glinting on water surfaces). To mitigate the effect of area differences across regions, we also normalised AF and BA values by the area of each region to obtain comparable fractions. By integrating LC with AF and BA data, we generated normalised AF/BA time-series visualisations, fire frequency and land-cover statistics and fire seasonality analyses.



2.3.2 Spatio-temporal hotspot analysis of fire occurrence

To examine the spatial clustering of fire occurrences, we assessed whether fire counts in spatial units were independent of neighbouring units using three types of spatial autocorrelation analysis applied to active fire points in the Middle East over the study period (Anselin, 1996). The spatial resolution for the fishnet grid was carefully selected after testing multiple options (5 km, 10 km and 20 km) (Text S1 and Figure S1.1, S1.2, S1.3). The 10 km grid cell size was selected as this provides an optimal balance between capturing local fire patterns and maintaining regional context. In addition, queen contiguity is selected for the spatial weight matrix as it includes spatial associations by considering all adjacent cells (including those sharing only a corner) as neighbours without inflating the analysis with correlations from spatially disconnected cells, First, we used Global Moran's I to examine whether fire occurrences are clustered, dispersed or random (Moran, 1950). The null hypothesis (H_0) states that fire occurrences are randomly distributed across the study area. The calculation is presented in Eq. (1).

$$I = \frac{n \sum_{i=1}^n \sum_{j=1}^n w_{i,j} z_i z_j}{S_0 \sum_{i=1}^n i} \quad (1)$$

Where z_i is the deviation of fire count for grid cell i from the mean fire count across all cells. $w_{i,j}$ is the spatial weight between grid cell i and j . n represents the total number of grid cells and S_0 denotes the sum all spatial weights. A positive z-score indicates that grid cells with similar fire counts (either high or low) tend to cluster; while a negative z-score indicates a dispersed pattern.

Second, emerging hotspot analysis (EHA) is employed to account for both temporal and spatial patterns of active fire hotspots. This is a method that combines the Getis-Ord G_i^* statistic and the Mann-Kendall trend test to detect spatial clusters and evaluate their temporal trends over time (Getis & Ord, 1992; Kendall, 1938; Mann, 1945). This method requires creation of a space-time cube, stored as a NetCDF (Network Common Data Form) that organises active data into a three-dimensional grid representing spatial locations across time steps. This space-time cube was constructed using $10 \text{ km} \times 10 \text{ km}$ cells (the spatial dimension), stacked for each calendar year from 2001 to 2022, and the time step is set to one year. Each 'bin' in this cube therefore stores the annual count of active fire detections for one cell-year combination. The Getis-Ord G_i^* statistic is applied to detect the locations of clusters, including clusters of high fire counts (hotspots) or low fire counts (cold spots). The Getis-Ord G_i^* statistic for each cell i (the count of the active fire points) is given by Eq. (2).

$$G_i^* = \frac{\sum_{j=1}^n w_{i,j} x_j - \bar{X} \sum_{j=1}^n w_{i,j}}{S \sqrt{\left[\frac{n \sum_{j=1}^n w_{i,j}^2 - \left(\sum_{j=1}^n w_{i,j} \right)^2}{n-1} \right]}} \quad (2)$$

Here, x_j denotes the fire counts at location j ; $w_{i,j}$ is the spatial weight between cell i and cell j (neighbouring cells) based on first-order queen contiguity; \bar{X} and S denote the global mean and standard deviation of all counts; and n is the total number of cells. The calculation generates a z-score and a corresponding p-value for each bin, indicating whether the bin is statistically



clustered relative to neighbouring bins within the same time period. The G_i^* statistic bin value represents the z-score and its statistical significance. Values of 3, 2 and 1 indicate statistically significant hotspots at the 99 per cent, 95 per cent and 90 per cent confidence levels, respectively; while values of -3, -2 and -1 indicate statistically significant cold spots at the same confidence levels.

265 The sequence of G_i^* z-scores for each cell constitutes a 22-year time series. The EHA then applies the Mann–Kendall trend test to the time series of each bin. A significant positive trend implies increasingly intense clustering, while a significant negative trend reflects the opposite. By combining the spatial clustering (G_i^*) with the temporal trend (Mann–Kendall test), each 10 km cell is categorised following the ArcGIS EHA typology as new, consecutive, intensifying, persistent, diminishing, sporadic, oscillating or historical hotspots (Table S1).

270 2.3.3 Burned area trend analysis

To analyse long-term BA patterns in the Middle East, we first aggregated MODIS BA (MCD64A1, 500 m resolution) pixels. The MODIS product classifies each 500 m pixel as burned or unburned, and aggregation was necessary to derive continuous BA values that are comparable across the large study region. For instance, if 40 out of 400 pixels were classified as burned, this represented 10 per cent of the grid cell area, equivalent to 10 km² of BA within that 100 km² cell. The 10 km spatial resolution was selected as it provides a suitable balance between capturing local fire activity and maintaining regional representativeness and it is consistent with the spatial unit applied in the AF hotspot analysis, where 10 km was shown to be an effective distance for detecting spatial patterns. Following spatial aggregation, monthly BA layers were further aggregated to annual BA; firstly to reduce 0 value redundancy, and secondly to highlight long-term fire extent rather than short-term variability.

280 We evaluated temporal trends in annual BA time series using the Mann–Kendall (MK) trend test over the 22-year period. The MK test is a non-parametric technique widely used in environmental sciences, as it does not require data to be normally distributed and is resistant to the influence of outliers (Karami & Tavakoli, 2025; Kazemzadeh et al., 2022; Kendall, 1938; Lanzante, 1996). The test evaluates whether there is a monotonic upward or downward trend in the data over time, without requiring the data to follow a normal distribution. In this analysis, we used a p-value threshold of 0.05 to determine the statistical significance of the trends. The Mann–Kendall statistic S is computed as Eq. (3):

$$S = \sum_{k=1}^{n-1} \sum_{j=k+1}^n \text{sgn}(x_j - x_k) \quad (3)$$

Where x_j and x_k represent pixel values at years j and k , respectively. The function $\text{sgn}(x_j - x_k)$ is defined as Eq. (4):

$$\text{sgn}(x_j - x_k) = \begin{cases} 1, & (x_j - x_k) > 0 \\ 0, & (x_j - x_k) = 0 \\ -1, & (x_j - x_k) < 0 \end{cases} \quad (4)$$



290 This formulation evaluates all possible pairs of observations across the time series (2001–2022), returning +1 when BA increases, –1 when BA decreases and 0 when no change is observed. Kendall’s tau ranges from –1 to +1, with positive values indicating increasing BA trends (more frequent or severe fires), negative values indicating decreasing trends, and values closer to either extreme reflecting stronger trends. In this study, Kendall’s tau values greater than 0.5 and less than –0.5 are defined as strong increasing or decreasing trends, respectively, while values between –0.5 and 0.5 indicate limited trends. These thresholds serve as the primary criteria for interpreting the trend results.

295 2.3.4 Correlation analysis

To investigate factors influencing fire occurrence and spread, we conducted correlation analyses between AF, BA and other relevant variables after applying data homogenisation and extracting their values to 10 km grid. (Table 1). A decision was made to use a non-directional measure of association to assess relationships between our potential factors and fire activity (BA and AF) due to the high complexity and variability of fire dynamics. In addition, correlation provides a simple, symmetrical way to screen variables and pinpoint the strongest bivariate relationships. Grids with no BA during the study period were excluded from this study, reducing the dataset from 31,602 to 14,642 cells. After removing rows with missing values, the final dataset contained 63,730 observations. We calculated Spearman’s rank correlation between annual BA and the selected variables as this is a non-parametric measure that does not assume a linear relationship between variables. As most fires occur in croplands and are intentionally set by humans, we separated the dataset into two versions; one including cropland BA, and one excluding it. This allows us to isolate and examine the extent to which climatic factors influence non-agricultural fires such as those occurring in forests and natural vegetation. In addition, we focused on areas containing the most significant BA trend pixels and AF hotspot grids and repeated the correlation analysis within these sub-areas in order to assess regional effect on variables influencing AF and BA.

3 Results

310 3.1 Fire activity patterns in the Middle East

Active fire (AF) and burned area (BA) and activity varied substantially across the eight study regions. While no BA was detected in Gaza due to coarse resolution of the BA product, one AF has been captured (Table 2, Figure 2, Table S2 and Figure S2). Regarding BA, Turkey, Iran and Iraq collectively dominate fire activity, accounting for 92 per cent of the total BA in the study area. Turkey alone contributes nearly half (48 per cent; mean annual BA of 5,257 km²), followed by Iran (23 per cent; 2,473 km² annually) and Iraq (21 per cent; 2,216 km² annually) (Table S2, Figure 3, Table S3, Figure S3). By contrast, Lebanon, Israel, the West Bank and Gaza exhibit only marginal fire occurrence, typically restricted to small, isolated areas. Regional variation in BA anomalies is significant; for instance, 2019 was a notable outlier for Syria (7,914 km²) and Iraq (15,396 km²), where the observed BA was nearly ten times the annual average (824 km² and 2,216 km², respectively; Table S3). Peak anomalies in other countries were more moderate and occurred in different years: Turkey in 2009, Iran and Israel in



320 2010, Lebanon in 2006 and the West Bank in 2015 (Table S3). Across the study area, croplands account for the majority of overall BA (74 per cent), followed by grasslands (16 per cent) and barren lands (5 per cent); except in Israel and Lebanon, where grasslands burned most frequently.

Table 2: Annual statistics per region, 2001–2022 (units: ‘km²’ for burned area, ‘count per 10 km²’ for active fire)

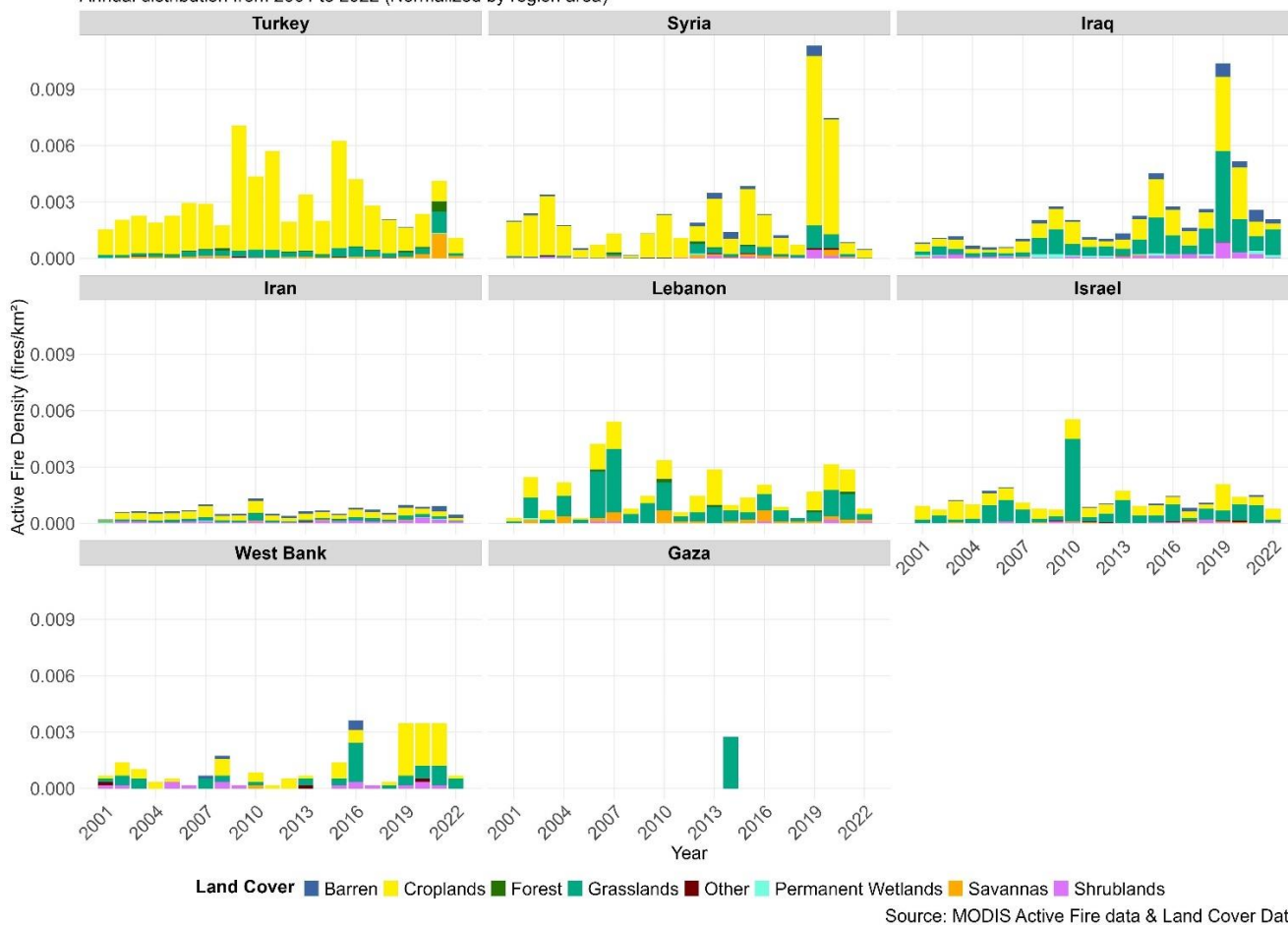
Statistics	Turkey	Syria	Iraq	Iran	Lebanon	Israel	West Bank	Gaza
Min. BA	2369	4.87	456	638	0	0.21	0	0
Mean BA	5253	824	2216	2473	3.54	15.2	2.09	0
Median BA	4270	296	1200	2283	0.68	12.9	1.09	0
Max. BA	12587	7913	15395	5582	14.9	54.5	8.11	0
Min. AF	1	1	1	1	1	1	1	1
Mean AF	3.78	3.35	3.64	2.71	1.66	1.8	1.45	1
Median AF	2	2	2	1	1	1	1	1
Max. AF	146	48	144	185	12	33	5	1

325 The normalised AF and ba confirm the fire anomaly in both Syria and Iraq in 2019, reaching exceptionally high burn fractions of approximately 4.0 per cent and 3.5 per cent of their country areas (Figure 2 and Figure 3). Furthermore, we identify differences between the two fire products; AF captures a more diverse range of land cover types and is able to detect smaller or fragmented fires that are missed by BA.



Active fire density by land cover type and region

Annual distribution from 2001 to 2022 (Normalized by region area)



Source: MODIS Active Fire data & Land Cover Data

330 **Figure 2: Normalised active fire counts by region and land cover type. The ‘Other’ class includes water bodies, urban and built-up areas and permanent snow and ice**

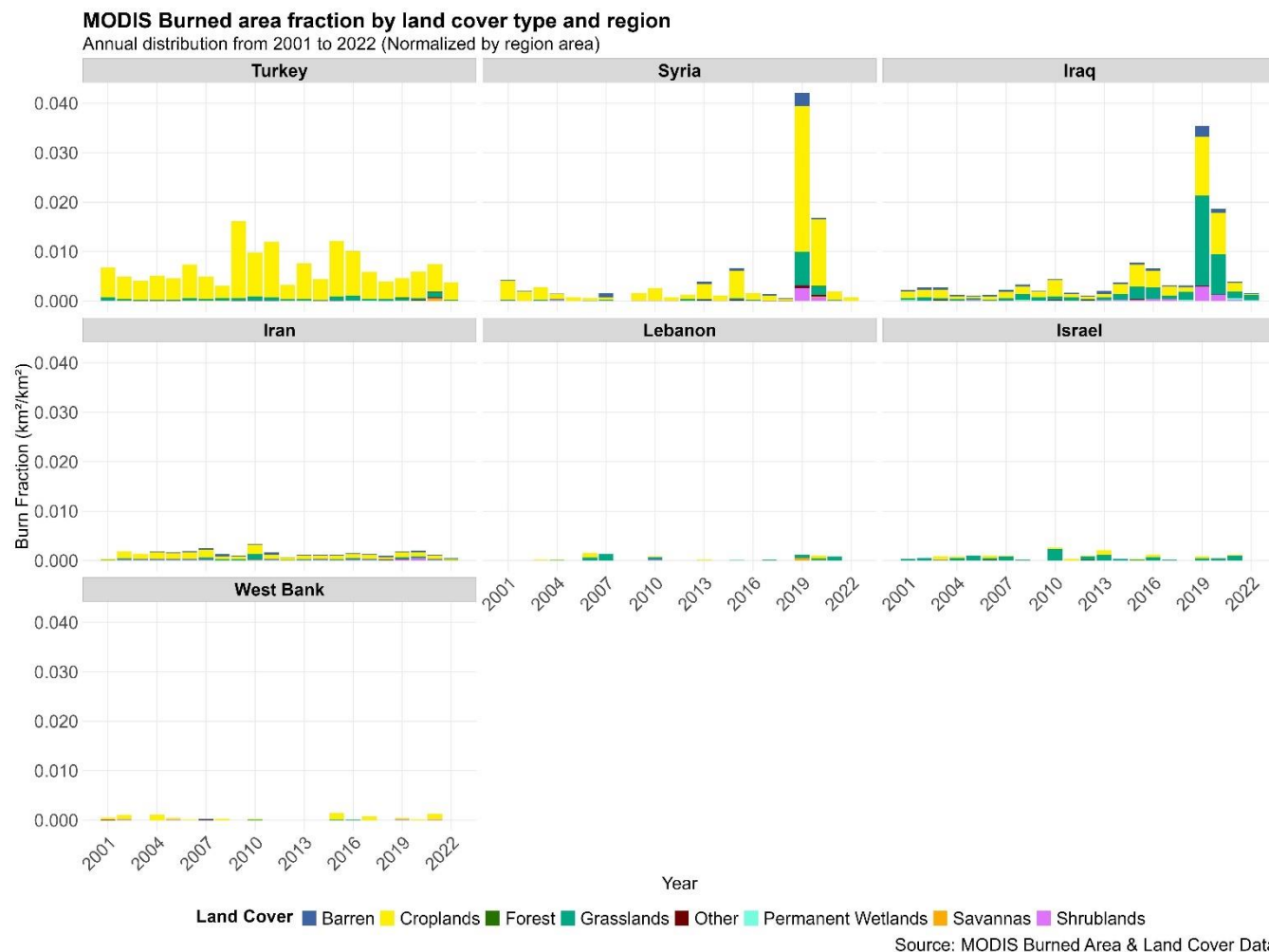


Figure 3: Normalised burned area by region and land cover type. The ‘Other’ class includes water bodies, urban and built-up areas and permanent snow and ice

335 **3.2 Fire frequency in different regions and land cover classes**

340 Fire frequency – the number of times each pixel burned during the study period – reveals repeated burn patterns across LC types and regions (Table 3). Iran shows the highest fire recurrence across multiple land cover classes, including open shrublands, savannas, grasslands, croplands and barren land. Turkey exhibits the most diverse fire occurrence patterns, with moderate to high frequencies across nearly all vegetation types. In contrast, the smaller territories of Palestine exhibit minimal fire activity across all LC types. In general, forest ecosystems exhibit lower fire frequencies across all regions, with mixed forests and deciduous broadleaf forests exhibiting the lowest fire occurrence.



Table 3: Fire frequency range for each land cover class and region (unit: number of pixels burned based on BA)

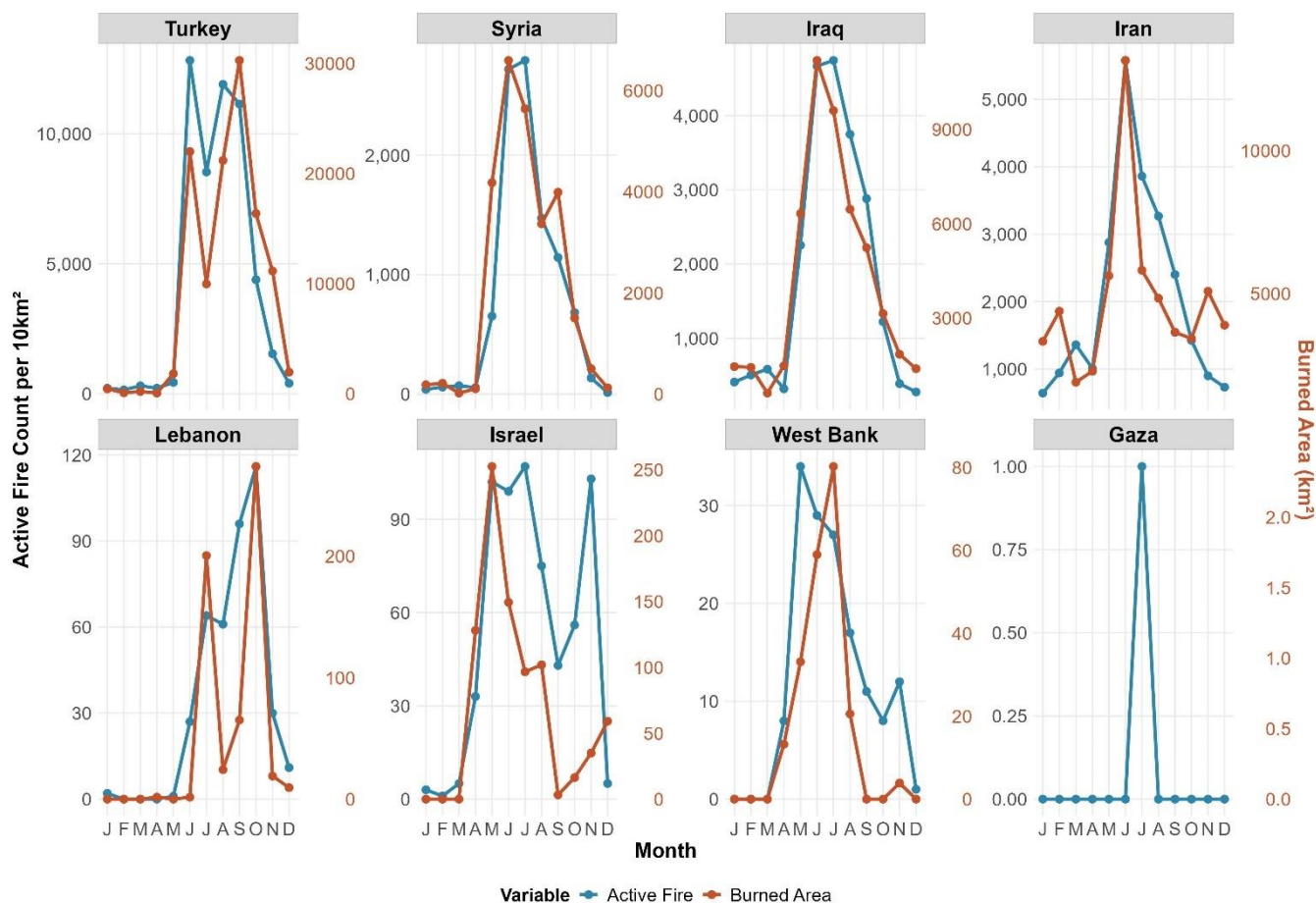
Land cover type	Turkey	Syria	Iraq	Iran	Lebanon	Israel	Gaza Strip	West Bank
Evergreen needleleaf forests	0–2	0–2	0	0	0–1	0	0	0
Deciduous broadleaf forests	0–1	0	0	0–3	0	0	0	0
Mixed forests	0–3	0	0	0–2	0	0	0	0
Open shrublands	0–12	0	0–8	0–19	0–1	0–1	0	0–1
Woody savannahs	0–2	0–2	0	0–5	0–0	0	0	0
Savannahs	0–13	0–2	0–4	0–9	0–1	0–1	0	0
Grasslands	0–9	0–3	0–12	0–16	0–2	0–7	0	0–2
Permanent wetlands	0–10	0–3	0–9	0–5	0–0	0	0	0
Croplands	0–29	0–12	0–16	0–20	0–2	0–3	0	0–5
Croplands/natural vegetation mosaics	0–4	0–2	0–1	0–2	0	0	0	0
Barren	0–6	0–4	0–16	0–16	0	0	0	0

345

3.3 Fire seasonality in different regions

Fire regimes can also be characterised through their AF and BA seasonality patterns (Figure 4). Both datasets reveal a consistent summer fire season across the study area, with peak activity concentrated between June and August. Most regions exhibit bimodal fire seasonality, with a primary summer peak and a secondary peak typically occurring in spring or autumn.

350 Overall, AF and BA show strong temporal agreement in larger countries such as Turkey, Syria, Iran and Iraq. However, the two datasets diverge in smaller or more heterogeneous landscapes such as Israel, with AF and BA exhibiting slightly different patterns in summer and autumn.



Source: MODIS Active Fire and Burned Area Data

Figure 4: Fire seasonality by region using AF and BA, based on monthly data from 2001 to 2022.

355 3.4 AF spatio-temporal hotspots

The Global Moran's I analysis yielded a significant p-value and a positive z-score, allowing us to reject the null hypothesis and confirming that fire occurrences are significantly clustered across the study area. Building on this, the EHA results reveal diverse AF hotspot patterns that can be classified into intensifying, persistent, sporadic and emerging spatio-temporal categories. These are represented by four sub-areas (A, B, C and D) characterised by prominent AF clusters (Figure 5).

360 Intensifying and persistent hotspots are most prominent in southern Turkey (Area C), where fire counts fluctuate between 500 and 2,500 annually. On the other hand, sporadic hotspots are primarily concentrated in southern Turkey (Areas B and C) and along the Iran–Iraq border (Area D). Area B has exhibited a decreasing trend since 2003, characterised by a prevalence of diminishing hotspots. In contrast, Area D along the Iran–Iraq border exhibits an increasing trend. Emerging hotspots can be observed in south-western Turkey (Area A), where a low-activity baseline was interrupted by a sharp surge exceeding 800 fire



365 counts in 2021, resulting in a concentrated cluster of new and consecutive hotspots. These results present an arc-shaped AF pattern that extends from western Turkey through northern Iraq to south-western Iran.

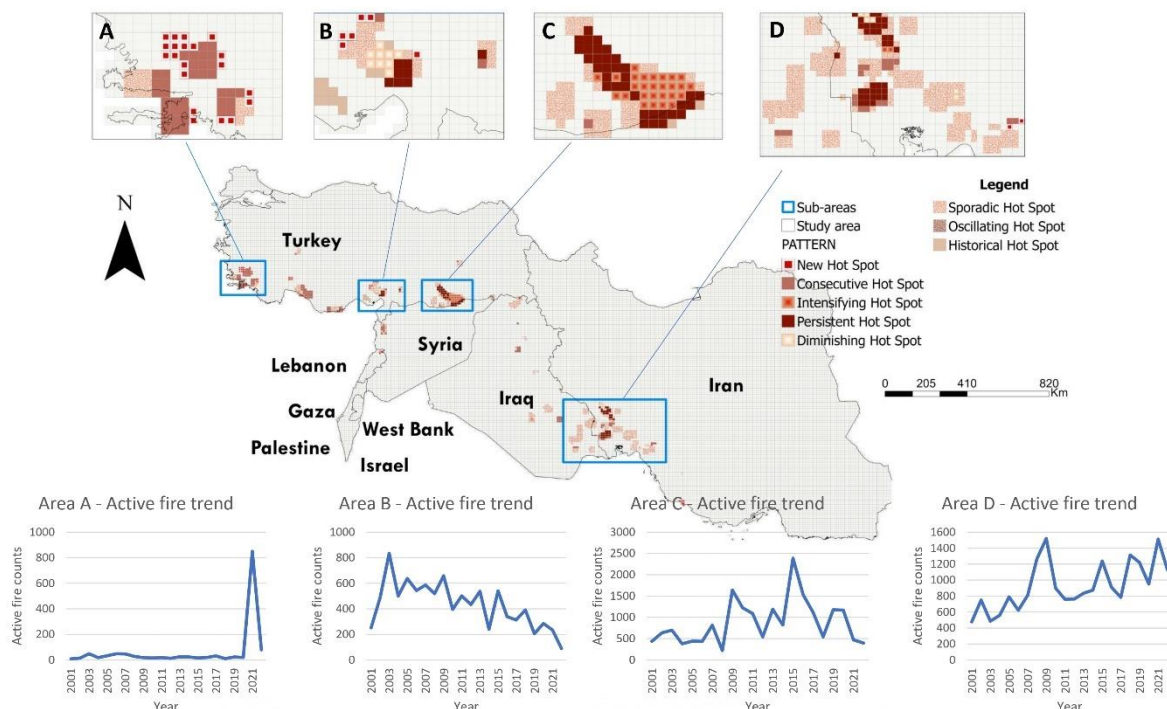
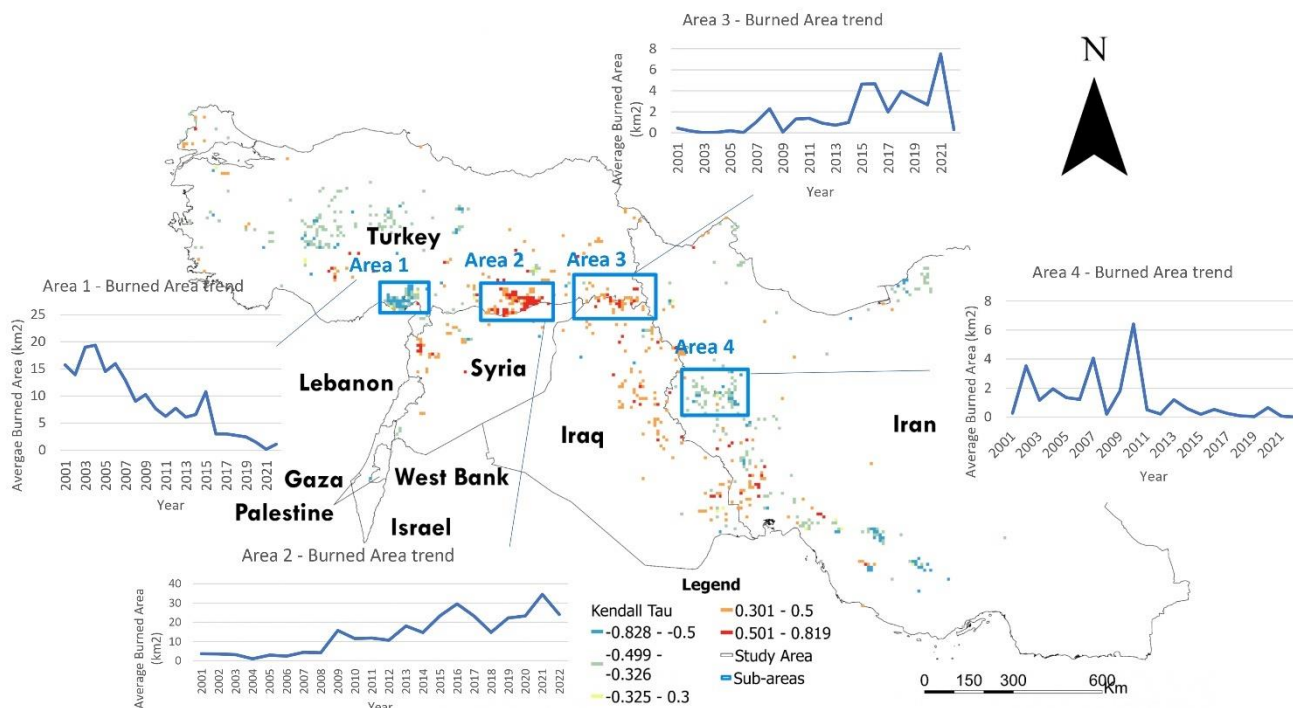


Figure 5: EHA results based on AF aggregated using a 10 km grid and a one-year time step. Time series plots show annual AF trends for four selected sub-areas (Areas A, B, C, D)

370 3.5 BA trend analysis results

The Mann-Kendall trend analysis results for annual BA between 2001 and 2022 reveal spatial patterns of significant increasing and decreasing trends across the region, exhibiting a similar but more continuous arc-shaped fire pattern compared to the AF EHA results (Figure 6). Four sub-areas (Area 1, Area 2, Area 3 and Area 4) have been selected as they reveal prevalent clusters of BA trends. Decreasing trends are observed in southern Turkey (Area 1), characterised by pixels with Kendall's tau values below -0.5. In contrast, significant increasing trends (Kendall's tau > 0.5) are identified in southern Turkey (Area 2), on the Turkey-Iraq border (Area 3) and in eastern Iraq. In western Iran (Area 4), fire activity was historically high but saw an abrupt decline following a major peak in 2010.



380 **Figure 6: BA trend analysis results based on annual BA between 2001 and 2022. Time series plots show annual burned area trends for four selected sub-areas (Areas 1, 2, 3, 4) with Mann-Kendall trend analysis results (Kendall’s tau values shown in legend).**

3.6 Spearman rank correlation

The Spearman rank correlation reveals a complex fire regime in the Middle East, illustrating the relationships between BA, AF and topographic, population, climatic and vegetation variables. The correlations between annual BA and explanatory variables are generally weak ($\rho < |0.2|$) but highly significant, suggesting that fire activity is not governed by any one variable. Instead, it is influenced by multiple interacting factors, potentially involving non-linearity and multi-causal relationships (Table 4).

Population density shows a significant positive correlation with BA, suggesting human influence on fire in this human-dominated landscape. Interestingly, the correlation coefficients remain remarkably similar regardless of whether croplands are included or excluded from the dataset; but there are fewer significant variables when croplands are excluded. Topographic variables show negative correlations with elevation ($\rho = -0.17$) and slope ($\rho = -0.18$), which indicates that larger BA values are more prevalent on flatter terrains and at lower elevations. Regarding climate, BA shows a significant positive correlation with SPEI during the wet season (such as mean, median and max. SPEI) and the twelve-month SPEI. These positive correlations suggest a moisture-driven fuel accumulation phenomenon, whereby wetter winters promote the growth of fine fuels that later facilitate the spread of fire during the dry season.



Table 4: Annual burned area correlation results including croplands (left). Annual burned area correlation results excluding croplands (right).

Spearman rank correlation with annual burned area (including croplands)			Spearman rank correlation with annual burned area (excluding croplands)		
Variable	Correlation coefficient	p-value	Variable	Correlation coefficient	p-value
elevation	-0.17137	0***	elevation	-0.17154	4E-224***
aspect	0.060936	2.33E-53***	aspect	0.004654	0.389429
slope	-0.18486	0***	slope	-0.11001	1.49E-92***
population	0.025434	1.42E-10***	population	0.0441	3.38E-16***
spei_wet_mean	0.064753	4.93E-60***	spei_wet_mean	0.020146	0.000195***
spei_wet_median	0.062265	1.23E-55***	spei_wet_median	0.01871	0.00054***
spei_wet_max	0.055274	3.32E-44***	spei_wet_max	0.023197	1.79E-05***
spei_wet_min	0.037142	7.44E-21***	spei_wet_min	-0.0024	0.657783
spei_dry_mean	-0.01249	0.00164**	spei_dry_mean	-0.00889	0.100073
spei_dry_median	-0.00983	0.013233*	spei_dry_median	-0.00838	0.12107
spei_dry_max	-0.01864	2.62E-06***	spei_dry_max	-0.00387	0.474411
spei_dry_min	0.012646	0.001431**	spei_dry_min	-0.0024	0.657783
spei12	0.036563	2.94E-20***	spei12	0.012791	0.018004*
Ndvi_sum	0.013708	0.000548***	Ndvi_sum	-0.00442	0.41388

*** indicates highly significant ($p < 0.0001$), ** indicates very significant ($p < 0.01$), * indicates significant ($p < 0.05$), . indicates marginally significant ($p < 0.01$)

400 The correlation analysis of the eight sub-areas (Areas A, B, C, D from the AF EHA and Areas 1, 2, 3, 4 from the BA trend analysis) reveals spatial heterogeneity (Figure 7). Their pattern can be classified into three fire regime types: Sect.3.6.1 Agricultural and flatland, Sect.3.6.2 Mountainous and transboundary, and Sect.3.6.3 Emergent forest.

3.6.1 Agricultural and flatland fire regime

405 This is located in southern Turkey (Areas 1 and B) and the Turkey–Syria border region (Areas 2 and C), where fire activity is concentrated in low-elevation croplands and shrublands. Despite their geographic proximity, these areas exhibit different responses to moisture. In southern Turkey, Area 1 (BA) exhibits a significant positive correlation with wet-season SPEI, while the overlapping Area B (AF) exhibits a negative relationship. Similarly, along the Turkey–Syria border, Area 2 (BA) displays a negative correlation with wet-season SPEI, in contrast to the positive correlation observed in the corresponding Area C (AF). This indicates that within the same localised region, BA and AF datasets respond differently to wet-season moisture variables.



410 **3.6.2 Mountainous and transboundary fire regime**

There are the areas along the Turkey–Syria–Iraq border (Area 3), the Zagros Mountains of western Iran (Area 4) and the Iraq–Iran border (Area D). In the Zagros Mountain area (Area 4), the positive correlation with wet-season SPEI and NDVI suggests that winter rainfall drives biomass growth, thereby providing fuel for summer fires. Conversely, the Iran–Iraq border (Area D) exhibits negative correlations with wet-season moisture and NDVI, indicating that the fire regime is limited more by aridity than by fuel availability. Along the Turkey–Syria–Iraq border (Area 3), fire activity exhibits negative correlations with both wet-season and dry-season SPEI, which indicates that warmer, drier conditions throughout the year promote fire expansion.

415

3.6.3 Emergent forest fire regime

This is characterised by western Turkey (Area A), which exhibited a low fire activity baseline prior to a sharp surge in 2021. While short-term wet-season moisture has limited influence here, fire occurrence is significantly correlated with long-term (twelve-month) and dry-season aridity, suggesting that prolonged drought and longer-term moisture accumulation are the primary drivers of fire in these Mediterranean forest and grassland systems.

420

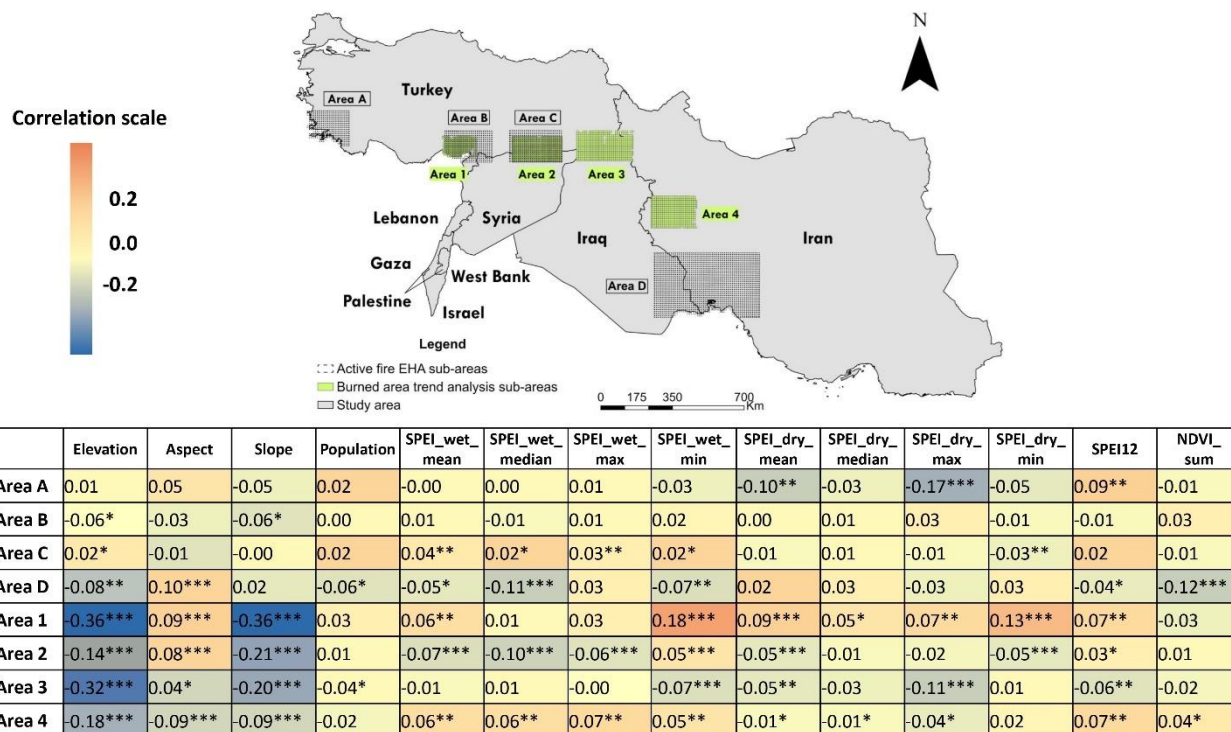


Figure 7: Spearman rank correlation coefficients between explanatory variables and BA (Areas 1, 2, 3, 4) and AF (Areas A, B, C, D). The panel on the left shows a correlation matrix with colour-coded values ranging from -0.36 (strong negative, blue) to +0.18 (moderate positive, orange). The bottom panel shows the geographic locations of study sub-areas. The analysis excludes areas with zero fire activity.

425



4 Discussion

This study provides a comprehensive analysis of AF and BA trends in the Middle East between 2001 and 2022, reflecting the interplay between biophysical factors (climate, topography, vegetation) and socio-economic factors (land use, population, regulations). Our findings yield four insights. First, we identify an arc-shaped transboundary fire pattern which extends across the Mediterranean towards the semi-arid steppe climate zone, along the borders of Turkey, Syria, Iraq and Iran, highlighting the importance of transboundary fire management. Second, we show that fire activities occur mostly in human-dominated landscapes, with croplands accounting for 74 per cent of the BA. Third, we found evidence for a ‘lagged climate effect’, whereby antecedent wet-season moisture assists fuel accumulation and promotes subsequent fire activity in several sub-areas. Fourth, our analysis shows the limitations of bivariate attribution in this region. The weak correlations between fire and single variables underscore the complexity of multi-causal fire regimes in which agricultural practices, land management and policy factors interact with biophysical conditions to shape fire activity.

4.1 Spatial and temporal variation in burned area and active fire

Our analysis shows that Turkey, Iraq and Iran have experienced the highest proportion of AF and BA across the region throughout the study period, due in part to the larger areas of these countries. Additionally, these countries possess the region’s most extensive belts of Mediterranean shrublands and fertile croplands, which serve as primary fuel sources. However, our findings indicate that a Mediterranean climate alone is not a reliable predictor of fire activity. Instead, the fire regime in the Mediterranean climate zone exhibits spatial heterogeneity, which suggests that factors such as topography, fuel types and human activities are also critical elements that alter the fire regime. Even within two climate regions, spatial heterogeneity marked by variations in elevation, temperature, precipitation and land cover (see Figure S4) creates distinct fire behaviour. Its influences on fire are further complicated by regional atmospheric phenomena, such as Mediterranean cyclones (Sirdas et al., 2017), and by diverse human activities such as cattle grazing (Lovreglio et al., 2014), agricultural residue burning (Hayran et al., 2018) and conflict-related activities (Dinc et al., 2021; Eklund & Dinc, 2024; Jaafar et al., 2022). These differences likely shaped the heterogeneity of fire dynamics in the region.

4.2 Fire anomaly warrants further investigation

We identified anomalous fire levels in Syria and Iraq in 2019 (Figure 2 and Figure 3), with 4 per cent of the total land area in Syria and 3.5 per cent in Iraq burned by fire during the year. This is consistent with the estimate reported by Zubkova et al. (2021), which found that 4.8 per cent of total land area in Syria was affected by fire.

The 2019 fires have been attributed to both climate anomalies and changes in socio-political stability, indicating the divergence of narratives around this event. Zubkova et al. (2021) attribute approximately 62 per cent of the surge to abnormal rainfall and high soil moisture, which boosted fuel loads in Syria. Jaafar et al. (2022), examining both Syria and Iraq, identify intentional ‘scorched earth’ arson by the Islamic State as a primary driver, sabotaging the water–food complex following its territorial



defeat. Schon et al. (2021), on the other hand, interpret the surge as a sign of ‘uneven stabilisation’ and agricultural renewal as populations returned to the land. Zubkova et al. (2021) argue that these fires actually exacerbated food insecurity and were
460 fuelled by conflict dynamics. Further research examining the fire dynamics of 2019 in Syria, Iraq and neighbouring countries could provide a better understanding of the drivers of fire activity in the Middle East.

Despite the magnitude of this event, Syria and Iraq are not highlighted as areas of significant change in our long-term AF and BA trend analysis (Figure 5, Figure 6) because the Mann-Kendall trend analysis algorithm is designed to detect continuous, monotonic increases or decreases in fire activity over the 22-year period; a singular, extreme fire anomaly hardly constitutes a
465 consistent trend. This interpretation is crucial for understanding that the 2019 fire anomaly does not alter the regional fire regime baseline.

4.3 Most burned area and active fire occurred on croplands

According to our findings, 74 per cent of the burned area occurred on croplands in the Middle East between 2001 and 2022. This aligns with data from the Global Fire Emissions Database (GFED5), which indicate that 80 per cent of BA occurs on
470 croplands (Chen et al., 2023), representing the highest global proportion of BA on croplands. Crop residue burning is a common agricultural practice in many countries worldwide, including in the Middle East, as this is a convenient and economically efficient method that can eliminate pests from the land (Çınar et al., 2025; Demirdogen, 2024; Hayran et al., 2018; Sabancı, 2025). This practice is illegal in Iran (Zargarani Khouzani & Dehghani Ghahfarokhi, 2022) and Turkey (Türkiye Forest Law No. 6831), and during parts of the year in Lebanon (Law No. 558 of 1996 on forest protection). The practice is known to cause
475 soil erosion and air pollution and increase the risk of spreading fire to adjacent forests and shrubs, posing risks to nearby populations (Çınar et al., 2025; Demirdogen, 2024; Yakupoğlu et al., 2022). In conflict-affected areas, these risks are compounded by the weaponisation of fire to destroy agricultural livelihoods (Eklund & Dinc, 2024; Jaafar et al., 2022). Despite evidence that farmers maintain positive attitudes toward sustainable agricultural practices, including alternatives to stubble burning (Hayran et al., 2018), many lack the capital for specialised harvesters, or the policy support needed to profit from
480 straw collection (Yusuf Özgür, 2025). Moreover, many farmers are unaware of the risks and negative impacts of stubble burning. These findings underscore the need for comprehensive agricultural waste management strategies, enhanced government subsidies and targeted education and communication to support a transition away from traditional burning towards more sustainable and lower-risk practices.

4.4 Fire seasonality patterns in Israel and Lebanon

485 Differences in fire seasonality across the region can be associated with precipitation patterns (dry and wet seasons), temperature regimes (hot and cool seasons) and agricultural practices. Although dual peaks appear in a number of areas, only Israel and Lebanon show distinct fire peaks in both the dry and wet seasons. In these areas, the fire regime is dominated less by agricultural cycles and more by transitional synoptic systems and seasonal climate variability, leading to bimodal fire seasonality.



490 In Israel, wildfires occur during the dry season (April to November), peaking in May to early July and October to early
November. These peaks coincide with hot, dry synoptic systems that bring hot and dry air from adjacent deserts, coupled with
strong winds associated with the Sharav Low (spring) and the Red Sea Trough (autumn) during the transitional seasons (Levin
& Heimowitz, 2012). Similarly, Lebanon exhibits an unusual bimodal fire season from June to November, with peak BA in
July and October; notably with minimal burning in August, which is unusual for the Mediterranean Basin. Based on
495 observations between 2001 and 2022, this late-season fire activity results from prolonged droughts, high wind speeds,
temperature extremes and low relative humidity, intensifying fire weather conditions in the autumn months (Majdalani et al.,
2022).

Both Israel and Lebanon experience a marked decrease in BA in August and September, but moderate fire activity can still be
detected by AF observations. In addition, Israel experiences a sharp increase in AF detections in November; however, BA
500 remains relatively low, suggesting a high frequency of small-scale fires that do not spread extensively. This divergence
highlights differences between the two fire datasets, indicating that they should be viewed as complementary.

4.5 Fire trend and transboundary patterns

The Mann-Kendall trend analysis identifies areas where BA exhibits a consistent monotonic increase or decrease, thereby
detecting statistically significant trend pixels. Consequently, regions such as north-western Iraq, where fire frequency is high
505 (Figure S4) but lacks sustained directional change, do not display clusters of significant pixels (Figure 6). In addition, the most
significant trends form a prominent arc-shaped pattern tracing the borders of Turkey, Syria, Iraq and Iran; this pattern is also
evident in the fire frequency map shown in Figure S4. This observation is consistent with Velayati et al. (2024), who identified
a high frequency of wildfires predominantly concentrated along the political borders of these countries, specifically in regions
such as Mardin (Turkey–Syria border) and Şırnak (Iraq–Syria–Turkey tri-border).

510 We observed a significant decreasing BA trend in the Çukurova Plain within Adana Province in southern Turkey (Area 1).
This finding aligns with Öztornacı (2024), who notes that growth in livestock activity in Adana has led to a reduction in double
cropping of wheat and maize in favour of forage crops and reports a negative correlation between livestock expansion and AF.
In contrast, the Kızıltepe Plain (Area 2) in Mardin Province in Turkey shows a stable increase in BA. Since 1989, the Southeast
Anatolia Project (known as GAP) has increased agricultural production in this area and further intensified the use of crop
515 residue burning (Bahşi et al., 2023). The study by Eklund & Thompson (2017) supports this finding, as productivity in this
region of Turkey remained stable, and even increased during the drought period between 2006 and 2010.

The northern segment of the regional ‘arc’ (Area 3), encompassing Zakho and Amedi in Iraq and Şemdinli in Turkey, has
exhibited an increasing trend since 2015 (Figure 6). Vegetation in this mountainous area comprises a mix of agricultural land,
pastures and forests. Eklund & Dinc (2024) found that AF hotspots and conflict events co-occurred in this area between 2016
520 and 2022, linked to armed conflicts between the Kurdistan Workers’ Party (PKK) and the Turkish armed forces.

Further east, in the Zagros Mountains (Area 4), our observations indicate a decreasing trend in BA, particularly following the
2010 peak. While Safdary et al., (2025) reported an increase in the number of individual AF detections from 2000 to 2019 in



parts of this region, our BA results suggest that the total area affected by large fires is declining, which may indicate a growing number of smaller fires in forests. In the northern borderlands (Marivan and Penjwen), there is a ‘fire corridor’ where more than 80 per cent of BA occurs within 5 km of the border (Rahimi et al., 2025). Fire management in this zone is severely constrained by landmines and unexploded ordnance dating back to the Iran–Iraq War of 1980–1988, posing lethal risks to emergency responders (Rahimi et al., 2025). In the southern borderland, the driver shifts to the ecological desiccation of the Hoor al-Azim wetlands caused by upstream dams and oil exploration. This drying process transforms the landscape into flammable tinder, fuelling intense transboundary wildfires that spread smoke across both countries (UNPO & AHRO, 2024). Whether through the presence of war remnants or the loss of wetlands, these segments illustrate how regional pressures generate shared crises requiring bilateral cooperation.

4.6 Correlation patterns in fire dynamics

The correlation analysis revealed generally weak associations between all variables and both AF and BA, even after exclusion of agricultural fires (Table 4). These weak bivariate relationships suggest a complex fire regime influenced by factors not explicitly captured in our correlation model. While population was the only socio-economic variable included, previous research in the region suggests linkages between fire and anthropogenic drivers such as stubble burning, grazing, and armed conflicts. We suggest further investigation into the socio-political dimension is essential for a thorough understanding of fire dynamics in this region.

Furthermore, the limited correlation may reflect mismatches in spatial scales. While climate variables such as precipitation and temperature influence fire weather at a regional level, fire occurrence is locally dependent on microclimatic conditions (such as fuel moisture and fuel temperature) and specific ignition sources. Our correlation model did not explicitly account for these scale mismatches, as the data were aggregated to a coarser level (10 km). This is consistent with findings from a study of forest fires in Lebanon, which also reported weak correlations between fire occurrence and relative humidity, precipitation and wind speed, attributing this to the non-linear and indirect influence of these variables on burning processes (Hamadeh et al., 2017).

Despite these overall weak trends, specific patterns emerged in Areas 1, 2, 3 and 4 which showed strong negative correlations between fire activity and both elevation and slope. This trend is directly linked to land-use patterns: agricultural productivity is predominantly concentrated in flat, low-lying areas (Eklund et al., 2016). Because these fertile lowlands are the primary sites for crop residue burning and managed fires, fire frequency naturally decreases as terrain becomes steeper and elevation increases. Thus, elevation and slope serve as geographical proxies for agricultural intensity rather than direct physical constraints on fire spread.

In addition, wetter conditions during wet seasons and drier conditions during dry seasons appear to promote fire activity slightly, with effects extending up to at least twelve months, as indicated by the correlation between SPEI12 and fire (Figure 7). This finding is consistent with the earlier research showing that fuel accumulation during antecedent wet periods can enhance subsequent fire spread and burned area (Ekberzade et al., 2025; Turco, Levin, et al., 2017). The relationship between



560 population density and fires has been widely discussed (Bistinas et al., 2013; Knorr et al., 2014). At very low population densities, fire activity is limited by insufficient ignitions. As population increases, burned area tends to rise due to human ignitions and agricultural burning, particularly in rangelands. However, fire suppression, landscape fragmentation and reduced fuel continuity limit burning at higher population densities. The relationship is therefore often non-monotonic, with burned area peaking at intermediate population densities (~7–10 people per km²) before declining (Bistinas et al., 2013). In this study, however, no clear pattern is perceived between population and fire, possibly because fire occurs mostly in sparsely populated croplands and forests, and because of uncertainties in population density data for rural areas (Láng-Ritter et al., 2025).

4.7 Data and method limitations

565 The study is subject to several limitations related to data quality and methodological constraints. First, MODIS AF and BA are the most widely used global fire datasets and are particularly valuable for monitoring fires in rural regions, along international borders and in conflict-affected zones where in-situ observations are unavailable. These two datasets are frequently paired because their detection methods complement one another; however, each dataset bears weaknesses that affect our analysis. Although MODIS BA uses AF detections to guide training sample selection and prior probabilities, the final burn mapping still relies on reflectance-based change detection (Giglio et al., 2009). As a result, not all AF detections correspond to burned-area pixels, and small or low-intensity fires may remain undetected. Data limitations are particularly evident in the Middle East, where the probability of detecting fires using the MODIS Collection 6 AF product is estimated to be just 7 per cent, the lowest among assessed regions globally (Giglio et al., 2016). Despite this low detection probability, the AF dataset remains suitable for capturing relative regional fire regimes, interannual variability and long-term fire trends because of its consistent and long-term temporal coverage across the Middle East.

575 Second, discrepancies between MODIS LC data and national statistics suggest potential misclassification issues. For example, MODIS LC classifies just 6 per cent (45,164 km²) of Turkey as forest in 2022, whereas Turkey's Ministry of Agriculture and Forestry reports 30 per cent (232,450 km²) forest cover in 2022 (General Directorate of Forestry (OGM), 2023). This discrepancy may affect fire attribution across land cover types. According to our results, most fires occurred on croplands, shrublands, grasslands and barren land, with just 0.3 per cent of BA in forests. Forest fires have nonetheless caused severe damage to livelihoods in the region (Acar & Gonencgil, 2023) and may be underestimated based on the LC data used in this study.

Third, the 10 km spatial resolution effectively captures broad patterns but misses small agricultural fires and local drivers that are obscured during aggregation. This also means that smaller burned areas and fire drivers, such as local land management practices, microclimatic conditions and small-scale topographic influences, cannot be adequately captured at this resolution.

585 Finally, the Spearman rank correlation model used in this study cannot fully capture the relationships between AF, BA and biophysical and population variables when the associations are non-linear, lagged or influenced by interactions with LC and local environmental conditions. Future work should incorporate a broader range of biophysical and anthropogenic variables, along with modelling approaches capable of representing these complex dynamics.



5 Conclusion

590 This study provides a comprehensive spatio-temporal analysis of fire dynamics across the Middle East from 2001 to 2022, revealing complex and heterogeneous patterns of vegetation fires. We found that croplands account for 74 per cent of total BA in the region. This finding indicates that agricultural practices effectively shape the regional fire regime. However, the prominent arc-shaped transboundary fire pattern along the borders of Turkey, Syria, Iraq and Iran highlights the fact that these fire regimes are not merely agricultural in nature, but also represent a transboundary management challenge across multiple
595 countries.

The weak correlations identified between fire activity and biophysical and population variables suggest that fire is not a simple linear response to climate or fuel. Instead, our findings indicate that fire patterns may be driven by factors beyond environmental thresholds examined in this study. As existing literature show the association between fire activities and political context, interpreting these fire patterns require wider socio-environmental framework. Such a framework highlights complex
600 human-environment interactions shaped by land use, fire management and regional political conditions, including armed conflict. This research contributes a regional, transboundary fire assessment of a conflict-affected dryland system, addressing a critical gap in the natural hazards literature. While this study identifies spatial and temporal patterns and potential factors influencing vegetation fires, it also highlights the limitations of regional scale analysis in capturing the precise motivations behind individual ignitions. Future research should adopt interdisciplinary frameworks that integrate these macro scale trends
605 with localised socio-environmental data. Expanding our understanding of these deeper socio-political drivers will support the future development of more resilient fire management strategies in the Middle East.

Code and data availability

The data used in this study are available at https://firms.modaps.eosdis.nasa.gov/active_fire/ (active fire data), https://developers.google.com/earth-engine/datasets/catalog/MODIS_061_MCD64A1 (burned area data),
610 <https://essd.copernicus.org/articles/15/5449/2023/> (SPEI data), <https://gee-community-catalog.org/projects/aster/> (topography data), https://developers.google.com/earth-engine/datasets/catalog/WorldPop_GP_100m_pop_age_sex_cons_unadj#description (population data), https://developers.google.com/earth-engine/datasets/catalog/MODIS_061_MCD12Q1 (land cover data), https://developers.google.com/earth-engine/datasets/catalog/MODIS_061_MOD13A1 , https://developers.google.com/earth-engine/datasets/catalog/MODIS_061_MYD13A1 (NDVI data). The codes facilitate the findings are provided at
615 supplementary material.

Supplement link

The link to the supplement will be included by Copernicus.



Author contributions

620 WL conceived the study, conducted the spatio-temporal, trend, emerging hotspot (EHA) and correlation analyses, produced all figures and led the writing of the manuscript. AHA contributed to the development of the trend analysis code, provided methodological guidance and contributed to the conceptualisation and writing of the study. LE contributed to the conceptualisation of the study and provided methodological guidance and editorial feedback.

Competing interests

625 There are no competing interests to declare.

Disclaimer

Publisher's note: Copernicus Publications remains neutral with regard to jurisdictional claims made in the text, published maps, institutional affiliations, or any other geographical representation in this paper. While Copernicus Publications makes every effort to include appropriate place names, the final responsibility lies with the authors. Views expressed in the text are those of the authors and do not necessarily reflect the views of the publisher.

630

Acknowledgements

The research was funded by the Swedish National Space Agency (grant 2022-00111 'Pyrogeography in Conflict Contexts: Satellite Remote Sensing of Vegetation Fires in the Middle East'). The research presented in this paper also contributes to the strategic research areas Biodiversity and Ecosystem Services in a Changing Climate (BECC) and The Middle East in the Contemporary World (MECW) at the Centre for Advanced Middle Eastern Studies, Lund University, Sweden. The authors used AI-based tools to assist with code refinement and language editing. All analyses, interpretations, and conclusions were developed and verified by the authors.

635

Review statement

The review statement will be added by Copernicus Publications listing the handling editor as well as all contributing referees according to their status anonymous or identified.

640



References

- Abel, C., Horion, S., Tagesson, T., De Keersmaecker, W., Seddon, A. W. R., Abdi, A. M., & Fensholt, R. (2020). The human–environment nexus and vegetation–rainfall sensitivity in tropical drylands. *Nature Sustainability*, 4(1), 25–32. <https://doi.org/10.1038/s41893-020-00597-z>
- 645 Abrams, M., Yamaguchi, Y., & Crippen, R. (2022). ASTER GLOBAL DEM (GDEM) VERSION 3. *The International Archives of the Photogrammetry, Remote Sensing and Spatial Information Sciences*, XLIII-B4-2022, 593–598. <https://doi.org/10.5194/isprs-archives-XLIII-B4-2022-593-2022>
- Acar, Z., & Gonencgil, B. (2023). Forest fires in southern Turkey July–August 2021. *Revista de Climatología*, 23, 46–57. <https://doi.org/10.59427/rcli/2023/v23.46-57>
- 650 AghaKouchak, A., Chiang, F., Huning, L. S., Love, C. A., Mallakpour, I., Mazdiyasi, O., Moftakhari, H., Papalexiou, S. M., Ragno, E., & Sadegh, M. (2020). Climate Extremes and Compound Hazards in a Warming World. *Annual Review of Earth and Planetary Sciences*, 48(1), 519–548. <https://doi.org/10.1146/annurev-earth-071719-055228>
- Andela, N., Morton, D. C., Giglio, L., Chen, Y., Van Der Werf, G. R., Kasibhatla, P. S., DeFries, R. S., Collatz, G. J., Hantson, S., Kloster, S., Bachelet, D., Forrest, M., Lasslop, G., Li, F., Mangeon, S., Melton, J. R., Yue, C., & Randerson, J. T. (2017). 655 A human-driven decline in global burned area. *Science*, 356(6345), 1356–1362. <https://doi.org/10.1126/science.aal4108>
- Anselin, L. (1996). *The Moran scatterplot as an ESDA tool to assess local instability in spatial association*. Fisher, M., Scholten, HJ and Unwin, DW (eds). *Spatial analytical perspectives in GIS*. Taylor&Francis. London. p.
- Ardakani, A. S., Zoj, M. J. V., Mohammadzadeh, A., & Mansourian, A. (2011). Spatial and Temporal Analysis of Fires Detected by MODIS Data in Northern Iran From 2001 to 2008. *IEEE Journal of Selected Topics in Applied Earth Observations and Remote Sensing*, 4(1), 216–225. <https://doi.org/10.1109/JSTARS.2010.2088111>
- 660 Aydin-Kandemir, F., & Demir, N. (2023). 2021 Turkey mega forest Fires: Biodiversity measurements of the IUCN Red List wildlife mammals in Sentinel-2 based burned areas. *Advances in Space Research*, 71(7), 3060–3075. <https://doi.org/10.1016/j.asr.2023.01.031>
- Bahşi, K., Ustaoglu, B., Aksoy, S., & Sertel, E. (2023). Estimation of emissions from crop residue burning in Türkiye using remotely sensed data and the Google Earth Engine platform. *Geocarto International*, 38(1), 2157052. <https://doi.org/10.1080/10106049.2022.2157052>
- Baudena, M., Santana, V. M., Baeza, M. J., Bautista, S., Eppinga, M. B., Hemerik, L., Garcia Mayor, A., Rodriguez, F., Valdecantos, A., Vallejo, V. R., Vasques, A., & Rietkerk, M. (2020). Increased aridity drives post-fire recovery of Mediterranean forests towards open shrublands. *New Phytologist*, 225(4), 1500–1515. <https://doi.org/10.1111/nph.16252>
- 670 Bilgili, E., & Saglam, B. (2003). Fire behavior in maquis fuels in Turkey. *Forest Ecology and Management*, 184(1–3), 201–207. [https://doi.org/10.1016/S0378-1127\(03\)00208-1](https://doi.org/10.1016/S0378-1127(03)00208-1)
- Bistinas, I., Oom, D., Sá, A. C. L., Harrison, S. P., Prentice, I. C., & Pereira, J. M. C. (2013). Relationships between Human Population Density and Burned Area at Continental and Global Scales. *PLoS ONE*, 8(12), e81188. <https://doi.org/10.1371/journal.pone.0081188>
- 675 Bondarenko, M., Kerr, D., Sorichetta, A., Tatem, A., & WorldPop. (2020). *Census/projection-disaggregated gridded population datasets for 51 countries across sub-Saharan Africa in 2020 using building footprints* [Data set]. <http://dx.doi.org/10.5258/SOTON/WP00682>
- Calviño-Cancela, M., Chas-Amil, M. L., García-Martínez, E. D., & Touza, J. (2017). Interacting effects of topography, vegetation, human activities and wildland-urban interfaces on wildfire ignition risk. *Forest Ecology and Management*, 397, 10–17. <https://doi.org/10.1016/j.foreco.2017.04.033>
- 680 Chen, Y., Hall, J., Van Wees, D., Andela, N., Hantson, S., Giglio, L., Van Der Werf, G. R., Morton, D. C., & Randerson, J. T. (2023). Multi-decadal trends and variability in burned area from the fifth version of the Global Fire Emissions Database (GFED5). *Earth System Science Data*, 15(11), 5227–5259. <https://doi.org/10.5194/essd-15-5227-2023>
- Chuvieco, E., Mouillot, F., Van Der Werf, G. R., San Miguel, J., Tanase, M., Koutsias, N., García, M., Yebra, M., Padilla, M., 685 Gitas, I., Heil, A., Hawbaker, T. J., & Giglio, L. (2019). Historical background and current developments for mapping burned area from satellite Earth observation. *Remote Sensing of Environment*, 225, 45–64. <https://doi.org/10.1016/j.rse.2019.02.013>
- Çınar, T., Cakır, M. F., & Aydın, A. (2025). Assessment of environmental and atmospheric impacts of stubble burning in Mardin-Diyarbakır (Southeastern of Türkiye): A remote sensing approach. *Natural Hazards*, 121(15), 17895–17912. <https://doi.org/10.1007/s11069-025-07496-6>



- 690 Demirdogen, A. (2024). Stubble burning: What determines this fire? *Environmental Development*, 51, 101029. <https://doi.org/10.1016/j.envdev.2024.101029>
- Dinc, P., Eklund, L., Shahpurwala, A., Mansourian, A., Aturinde, A., & Pilesjö, P. (2021). Fighting Insurgency, Ruining the Environment: The Case of Forest Fires in the Dersim Province of Turkey. *Human Ecology*, 49(4), 481–493. <https://doi.org/10.1007/s10745-021-00243-y>
- 695 Ekberzade, B., Görüm, T., Karabacak, F., Akay, S. S., & Şen, Ö. L. (2025). Up in flames: The human factor behind a megafire in Mediterranean Türkiye. *Npj Natural Hazards*, 2(1), 65. <https://doi.org/10.1038/s44304-025-00120-4>
- Eklund, L., Abdi, A. M., Shahpurwala, A., & Dinc, P. (2021). On the Geopolitics of Fire, Conflict and Land in the Kurdistan Region of Iraq. *Remote Sensing*, 13(8), 1575. <https://doi.org/10.3390/rs13081575>
- Eklund, L., & Dinc, P. (2024). Fires as collateral or means of war: Challenges of environmental peacebuilding in the Kurdistan Region of Iraq. *Ecology and Society*, 29(3), art25. <https://doi.org/10.5751/ES-15316-290325>
- 700 Eklund, L., Persson, A., & Pilesjö, P. (2016). Cropland changes in times of conflict, reconstruction, and economic development in Iraqi Kurdistan. *Ambio*, 45(1), 78–88. <https://doi.org/10.1007/s13280-015-0686-0>
- Eklund, L., & Thompson, D. (2017). Differences in resource management affects drought vulnerability across the borders between Iraq, Syria, and Turkey. *Ecology and Society*, 22(4), art9. <https://doi.org/10.5751/ES-09179-220409>
- 705 Ertugrul, M., Varol, T., Ozel, H. B., Cetin, M., & Sevik, H. (2021). Influence of climatic factor of changes in forest fire danger and fire season length in Turkey. *Environmental Monitoring and Assessment*, 193(1), 28. <https://doi.org/10.1007/s10661-020-08800-6>
- Eskandari, S., & Chuvieco, E. (2015). Fire danger assessment in Iran based on geospatial information. *International Journal of Applied Earth Observation and Geoinformation*, 42, 57–64. <https://doi.org/10.1016/j.jag.2015.05.006>
- 710 Friedl, M. A., & Sulla-Menasse, D. (2022). *MODIS/Terra+Aqua Land Cover Type Yearly L3 Global 500m SIN Grid V061* [Data set]. <https://doi.org/10.5067/MODIS/MCD12Q1.061>
- Frumkin, A., & Shtober-Zisu, N. (Eds). (2024). *Landscapes and Landforms of Israel*. Springer International Publishing. <https://doi.org/10.1007/978-3-031-44764-8>
- Gandham, H., Dasari, H. P., Luong, T. M., Attada, R., Hassan, W. U., Gopinathan, P. A., Saharwardi, M. S., & Hoteit, I. (2025). Declining summer circulation over the Eastern Mediterranean and Middle East. *Npj Climate and Atmospheric Science*, 8(1), 177. <https://doi.org/10.1038/s41612-025-01072-2>
- Gebrechorkos, S. H., Peng, J., Dyer, E., Miralles, D. G., Vicente-Serrano, S. M., Funk, C., Beck, H. E., Asfaw, D. T., Singer, M. B., & Dadson, S. J. (2023). Global high-resolution drought indices for 1981–2022. *Earth System Science Data*, 15(12), 5449–5466. <https://doi.org/10.5194/essd-15-5449-2023>
- 720 Genç, Ç. Ö., Küçük, Ö., Keleş, S. Ö., & Ünal, S. (2023). Burn severity evaluation in black pine forests with topographical factors using Sentinel-2 in Kastamonu, Türkiye. *CERNE*, 29, e-103230. <https://doi.org/10.1590/01047760202329013230>
- General Directorate of Forestry (OGM). (2023). *Forestry Statistics 2022* [Official Statistics]. Ormançılık İstatistikleri 2022 [Forestry Statistics 2022]. <https://www.ogm.gov.tr/tr/e-kutuphane/resmi-istatistikler>
- Getis, A., & Ord, J. K. (1992). The Analysis of Spatial Association by Use of Distance Statistics. *Geographical Analysis*, 24(3), 189–206. <https://doi.org/10.1111/j.1538-4632.1992.tb00261.x>
- 725 Giglio, L., Loboda, T., Roy, D. P., Quayle, B., & Justice, C. O. (2009). An active-fire based burned area mapping algorithm for the MODIS sensor. *Remote Sensing of Environment*, 113(2), 408–420. <https://doi.org/10.1016/j.rse.2008.10.006>
- Giglio, L., Schroeder, W., & Justice, C. O. (2016). The collection 6 MODIS active fire detection algorithm and fire products. *Remote Sensing of Environment*, 178, 31–41. <https://doi.org/10.1016/j.rse.2016.02.054>
- 730 Gorelick, N., Hancher, M., Dixon, M., Ilyushchenko, S., Thau, D., & Moore, R. (2017). Google Earth Engine: Planetary-scale geospatial analysis for everyone. *Remote Sensing of Environment*, 202, 18–27. <https://doi.org/10.1016/j.rse.2017.06.031>
- Guk, E., Bar-Massada, A., & Levin, N. (2023). Constructing a Comprehensive National Wildfire Database from Incomplete Sources: Israel as a Case Study. *Fire*, 6(4), 131. <https://doi.org/10.3390/fire6040131>
- Hamadeh, N., Karouni, A., Daya, B., & Chauvet, P. (2017). Using correlative data analysis to develop weather index that estimates the risk of forest fires in Lebanon & Mediterranean: Assessment versus prevalent meteorological indices. *Case Studies in Fire Safety*, 7, 8–22. <https://doi.org/10.1016/j.csfs.2016.12.001>
- 735 Hawbaker, T. J., Radeloff, V. C., Syphard, A. D., Zhu, Z., & Stewart, S. I. (2008). Detection rates of the MODIS active fire product in the United States. *Remote Sensing of Environment*, 112(5), 2656–2664. <https://doi.org/10.1016/j.rse.2007.12.008>



- 740 Hayran, S., Gul, A., & Ali Saridas, M. (2018). FARMERS' SUSTAINABLE AGRICULTURE PERCEPTION IN TURKEY: THE CASE OF MERSIN PROVINCE. *New Medit*, *XVII*(3), 69–78. <https://doi.org/10.30682/nm1803f>
- Jaafar, H., Sujud, L., & Woertz, E. (2022). Scorched earth tactics of the “Islamic State” after its loss of territory: Intentional burning of farmland in Iraq and Syria. *Regional Environmental Change*, *22*(4), 120. <https://doi.org/10.1007/s10113-022-01976-2>
- 745 Jahromi, M. N., Jahromi, M. N., Pourghasemi, H. R., Zand-Parsa, S., & Jamshidi, S. (2021). Chapter 12—Accuracy assessment of forest mapping in MODIS land cover dataset using fuzzy set theory. *Forest Resources Resilience and Conflicts*, 165–183.
- Jain, P., Coogan, S. C. P., Subramanian, S. G., Crowley, M., Taylor, S., & Flannigan, M. D. (2020). A review of machine learning applications in wildfire science and management. *Environmental Reviews*, *28*(4), 478–505. <https://doi.org/10.1139/er-2020-0019>
- 750 Jones, M. W., Abatzoglou, J. T., Veraverbeke, S., Andela, N., Lasslop, G., Forkel, M., Smith, A. J. P., Burton, C., Betts, R. A., Van Der Werf, G. R., Sitch, S., Canadell, J. G., Santín, C., Kolden, C., Doerr, S. H., & Le Quéré, C. (2022). Global and Regional Trends and Drivers of Fire Under Climate Change. *Reviews of Geophysics*, *60*(3), e2020RG000726. <https://doi.org/10.1029/2020RG000726>
- Karami, P., & Tavakoli, S. (2025). Non-parametric spatiotemporal trends in fire: An approach to identify fire regimes variations and predict seasonal effects of fire in Iran. *PLOS ONE*, *20*(4), e0319993. <https://doi.org/10.1371/journal.pone.0319993>
- 755 Katagis, T., & Gitas, I. Z. (2022). Assessing the Accuracy of MODIS MCD64A1 C6 and FireCCI51 Burned Area Products in Mediterranean Ecosystems. *Remote Sensing*, *14*(3), 602. <https://doi.org/10.3390/rs14030602>
- Kazemzadeh, M., Noori, Z., Jamali, S., & Abdi, A. M. (2022). Forty Years of Air Temperature Change over Iran Reveals Linear and Nonlinear Warming. *Journal of Meteorological Research*, *36*(3), 462–477. <https://doi.org/10.1007/s13351-022-1184-5>
- 760 Kendall, M. G. (1938). A New Measure of Rank Correlation. *Biometrika*, *30*(1–2). <https://doi.org/10.1093/biomet/30.1-2.81>
- Khwarahm, N. R. (2021). Spatial modeling of land use and land cover change in Sulaimani, Iraq, using multitemporal satellite data. *Environmental Monitoring and Assessment*, *193*(3), 148. <https://doi.org/10.1007/s10661-021-08959-6>
- 765 Kint, V., Aertsens, W., Fyllas, N. M., Trabucco, A., Janssen, E., Özkan, K., & Muys, B. (2014). Ecological traits of Mediterranean tree species as a basis for modelling forest dynamics in the Taurus mountains, Turkey. *Ecological Modelling*, *286*, 53–65. <https://doi.org/10.1016/j.ecolmodel.2014.04.023>
- Knorr, W., Kaminski, T., Arneth, A., & Weber, U. (2014). Impact of human population density on fire frequency at the global scale. *Biogeosciences*, *11*(4), 1085–1102. <https://doi.org/10.5194/bg-11-1085-2014>
- 770 Koutsias, N., Xanthopoulos, G., Founda, D., Xystrakis, F., Nioti, F., Pleniou, M., Mallinis, G., & Arianoutsou, M. (2013). On the relationships between forest fires and weather conditions in Greece from long-term national observations (1894–2010). *International Journal of Wildland Fire*, *22*(4), 493. <https://doi.org/10.1071/WF12003>
- Láng-Ritter, J., Keskinen, M., & Tenkanen, H. (2025). Global gridded population datasets systematically underrepresent rural population. *Nature Communications*, *16*(1), 2170. <https://doi.org/10.1038/s41467-025-56906-7>
- 775 Lanzante, J. R. (1996). RESISTANT, ROBUST AND NON-PARAMETRIC TECHNIQUES FOR THE ANALYSIS OF CLIMATE DATA: THEORY AND EXAMPLES, INCLUDING APPLICATIONS TO HISTORICAL RADIOSONDE STATION DATA. *International Journal of Climatology*, *16*(11), 1197–1226. [https://doi.org/10.1002/\(SICI\)1097-0088\(199611\)16:11%253C1197::AID-JOC89%253E3.0.CO;2-L](https://doi.org/10.1002/(SICI)1097-0088(199611)16:11%253C1197::AID-JOC89%253E3.0.CO;2-L)
- Levin, N., & Heimowitz, A. (2012). Mapping spatial and temporal patterns of Mediterranean wildfires from MODIS. *Remote Sensing of Environment*, *126*, 12–26. <https://doi.org/10.1016/j.rse.2012.08.003>
- 780 Li, X., Messina, J. P., Moore, N. J., Fan, P., & Shortridge, A. M. (2017). MODIS land cover uncertainty in regional climate simulations. *Climate Dynamics*, *49*(11–12), 4047–4059. <https://doi.org/10.1007/s00382-017-3563-7>
- Lovreglio, R., Meddour-Sahar, O., & Leone, V. (2014). Goat grazing as a wildfire prevention tool: A basic review. *iForest - Biogeosciences and Forestry*, *7*(4), 260–268. <https://doi.org/10.3832/ifer1112-007>
- 785 Majdalani, G., Koutsias, N., Faour, G., Adjizian-Gerard, J., & Mouillot, F. (2022). Fire Regime Analysis in Lebanon (2001–2020): Combining Remote Sensing Data in a Scarcely Documented Area. *Fire*, *5*(5), 141. <https://doi.org/10.3390/fire5050141>
- Mann, H. B. (1945). Nonparametric Tests Against Trend. *Econometrica*, *13*(3), 245–259. JSTOR. <https://doi.org/10.2307/1907187>



- Marriner, N. (2013). Fire in Mediterranean Ecosystems: Ecology, evolution and management: J.E. KEELEY, W.J. BOND, R.A. BRADSTOCK, J.G. PAUSAS, P.W. RUNDEL, (2012), Cambridge University Press, 515 p. *Méditerranée*, (121), 111.
790 <https://doi.org/10.4000/mediterranee.6936>
- McEvoy, D. J., Hobbins, M., Brown, T. J., VanderMolen, K., Wall, T., Huntington, J. L., & Svoboda, M. (2019). Establishing Relationships between Drought Indices and Wildfire Danger Outputs: A Test Case for the California-Nevada Drought Early Warning System. *Climate*, 7(4), 52. <https://doi.org/10.3390/cli7040052>
- Memisoglu Baykal, T. (2023). GIS-BASED spatiotemporal analysis of forest fires in Turkey from 2010 to 2020. *Transactions in GIS*, 27(5), 1289–1317. <https://doi.org/10.1111/tgis.13066>
795
- Mermoz, M., Kitzberger, T., & Veblen, T. T. (2005). LANDSCAPE INFLUENCES ON OCCURRENCE AND SPREAD OF WILDFIRES IN PATAGONIAN FORESTS AND SHRUBLANDS. *Ecology*, 86(10), 2705–2715. <https://doi.org/10.1890/04-1850>
- Moran, P. A. (1950). Notes on continuous stochastic phenomena. *Biometrika*, 37(1/2), 17–23.
- 800 Ne'eman, G., & Osem, Y. (Eds). (2021). *Pines and Their Mixed Forest Ecosystems in the Mediterranean Basin* (Vol. 38). Springer International Publishing. <https://doi.org/10.1007/978-3-030-63625-8>
- Novo, A., Dotal, H., & Eskandari, S. (2024). Fire susceptibility modeling and mapping in Mediterranean forests of Turkey: A comprehensive study based on fuel, climatic, topographic, and anthropogenic factors. *Euro-Mediterranean Journal for Environmental Integration*, 9(2), 655–679. <https://doi.org/10.1007/s41207-024-00475-6>
- 805 Öztornacı, B. (2024). The relationship between agricultural fires and livestock farming. *Heliyon*, 10(22), e40455. <https://doi.org/10.1016/j.heliyon.2024.e40455>
- Pellizzaro, G., Cesaraccio, C., Duce, P., Ventura, A., & Zara, P. (2007). Relationships between seasonal patterns of live fuel moisture and meteorological drought indices for Mediterranean shrubland species. *International Journal of Wildland Fire*, 16(2), 232–241. <https://doi.org/10.1071/WF06081>
- 810 Pilliod, D. S., Welty, J. L., & Arkle, R. S. (2017). Refining the cheatgrass–fire cycle in the Great Basin: Precipitation timing and fine fuel composition predict wildfire trends. *Ecology and Evolution*, 7(19), 8126–8151. <https://doi.org/10.1002/ece3.3414>
- Rahimi, I., Duarte, L., & Teodoro, A. C. (2025). Administrative borders and environmental change: A GIS and remote sensing approach to understanding forest fires in disputed territories. In K. Schulz, K. G. Nikolakopoulos, U. Michel, A. C. Teodoro, & V. Gagliardi (Eds), *Earth Resources and Environmental Remote Sensing/GIS Applications XVI* (p. 52). SPIE.
815 <https://doi.org/10.1117/12.3069720>
- Rasooli, S. B., Rashidi, S., & Shabani, N. (2021). Fire sensitivity of broadleaf tree species in plantations of Kurdistan, Iran. *Journal of Forestry Research*, 32(3), 1167–1176. <https://doi.org/10.1007/s11676-020-01185-9>
- Rousta, I., Olafsson, H., Nasserzadeh, M. H., Zhang, H., Krzyszczyk, J., & Baranowski, P. (2021). Dynamics of Daytime Land Surface Temperature (LST) Variabilities in the Middle East Countries During 2001–2018. *Pure and Applied Geophysics*, 178(6), 2357–2377. <https://doi.org/10.1007/s00024-021-02765-4>
820
- Sabancı, S. (2025). Climatic, geomorphological, and anthropogenic drivers of rural wildfires: A remote sensing and GIS-based case study of the June 2024 Diyarbakır-Mardin events-Türkiye. *International Journal of Disaster Risk Reduction*, 131, 105874. <https://doi.org/10.1016/j.ijdrr.2025.105874>
- Sadeghi, A., Ahmadi Nadoushan, M., & Ahmadi Sani, N. (2025). Drivers of wildfire spatial expansion: Modeling insights from semi-arid oak forests of W Iran. *Advances in Space Research*, 75(10), 7184–7194. <https://doi.org/10.1016/j.asr.2025.03.002>
825
- Safdary, R., Monavari, S. M., Babaie Kafaky, S., & Kiadaliri, H. (2025). The effect of spatiotemporal characteristics of drought and wet years on the development of fire occurrence in natural regions of western Iran (Lorestan Province). *Environmental Monitoring and Assessment*, 197(4), 398. <https://doi.org/10.1007/s10661-025-13843-8>
- 830 Salis, M., Laconi, M., Ager, A. A., Alcasena, F. J., Arca, B., Lozano, O., Fernandes De Oliveira, A., & Spano, D. (2016). Evaluating alternative fuel treatment strategies to reduce wildfire losses in a Mediterranean area. *Forest Ecology and Management*, 368, 207–221. <https://doi.org/10.1016/j.foreco.2016.03.009>
- Schon, J., Mezuman, K., Heslin, A., Field, R. D., & Puma, M. J. (2021). How fire patterns reveal uneven stabilization at the end of conflict: Examining Syria's unusual fire year in 2019. *Environmental Research Letters*, 16(4), 044046.
835 <https://doi.org/10.1088/1748-9326/abe327>



- Seydi, S. T., Abatzoglou, J. T., Jones, M. W., Kolden, C. A., Filippelli, G., Hurteau, M. D., AghaKouchak, A., Luce, C. H., Miao, C., & Sadegh, M. (2025). Increasing global human exposure to wildland fires despite declining burned area. *Science*, 389, 826–829.
- 840 Sirdas, S. A., Tuncay Özdemir, E., Sezen, İ., Efe, B., & Kumar, V. (2017). Devastating extreme Mediterranean cyclone's impacts in Turkey. *Natural Hazards*, 87(1), 255–286. <https://doi.org/10.1007/s11069-017-2762-1>
- The Unrepresented Nations and Peoples Organization (UNPO), & The Ahwaz Human Rights Organization (AHRO). (2024, September). *Water and Environmental Crisis in Hur al-Azim Wetland in Khuzestan Al-Ahwaz*.
- Thomson, D. R., Leasure, D. R., Bird, T., Tzavidis, N., & Tatem, A. J. (2022). How accurate are WorldPop-Global-Unconstrained gridded population data at the cell-level?: A simulation analysis in urban Namibia. *PLOS ONE*, 17(7), e0271504. <https://doi.org/10.1371/journal.pone.0271504>
- 845 Turco, M., Levin, N., Tessler, N., & Saaroni, H. (2017). Recent changes and relations among drought, vegetation and wildfires in the Eastern Mediterranean: The case of Israel. *Global and Planetary Change*, 151, 28–35. <https://doi.org/10.1016/j.gloplacha.2016.09.002>
- Turco, M., Von Hardenberg, J., AghaKouchak, A., Llasat, M. C., Provenzale, A., & Trigo, R. M. (2017). On the key role of 850 droughts in the dynamics of summer fires in Mediterranean Europe. *Scientific Reports*, 7(1), 81. <https://doi.org/10.1038/s41598-017-00116-9>
- Velayati, A. H., Boloorani, A. D., Kiavarz, M., Samani, N. N., & Alavipanah, S. K. (2024). Spatiotemporal analysis of wildfire in the Tigris and Euphrates basin: A remote sensing based wildfire potential mapping. *Remote Sensing Applications: Society and Environment*, 34, 101150. <https://doi.org/10.1016/j.rsase.2024.101150>
- 855 Vicente-Serrano, S. M., Beguería, S., & López-Moreno, J. I. (2010). A Multiscalar Drought Index Sensitive to Global Warming: The Standardized Precipitation Evapotranspiration Index. *Journal of Climate*, 23(7), 1696–1718. <https://doi.org/10.1175/2009JCLI2909.1>
- Wittenberg, L., & Kutiel, H. (2016). Dryness in a Mediterranean-type climate – implications for wildfire burnt area: A case study from Mount Carmel, Israel. *International Journal of Wildland Fire*, 25(5), 579. <https://doi.org/10.1071/WF15135>
- 860 Yakupoğlu, T., DiNdaroglu, T., RodriGo-ComiNo, J., & Cerdà, A. (2022). Stubble burning and wildfires in Turkey considering the Sustainable Development Goals of the United Nations. *EURASIAN JOURNAL OF SOIL SCIENCE (EJSS)*, 11(1), 66–76. <https://doi.org/10.18393/ejss.993611>
- Yusuf Özgür, B. (2025, March 18). Stubble burning in Anatolia: A farming practice undermining biodiversity and soil fertility. *Platform for Independent Journalism (P24)*. <https://platform24.org/en/articles/stubble-burning-in-anatolia/>
- 865 Zargaran Khouzani, M. R., & Deghani Ghahfarokhi, Z. (2022). Evaluation of Agricultural Waste Management Mechanism in Iran. *Industrial and Domestic Waste Management*, 2(2), 113–124. <https://doi.org/10.53623/idwm.v2i2.112>
- Zittis, G., Almazroui, M., Alpert, P., Ciais, P., Cramer, W., Dahdal, Y., Fnais, M., Francis, D., Hadjinicolaou, P., Howari, F., Jrrar, A., Kaskaoutis, D. G., Kulmala, M., Lazoglou, G., Mihalopoulos, N., Lin, X., Rudich, Y., Sciare, J., Stenchikov, G., ... Lelieveld, J. (2022). Climate Change and Weather Extremes in the Eastern Mediterranean and Middle East. *Reviews of Geophysics*, 60(3), e2021RG000762. <https://doi.org/10.1029/2021RG000762>
- 870 Zubkova, M., Giglio, L., Humber, M. L., Hall, J. V., & Ellicott, E. (2021). Conflict and Climate: Drivers of Fire Activity in Syria in the Twenty-First Century. *Earth Interactions*, 25(1), 119–135. <https://doi.org/10.1175/EI-D-21-0009.1>